

Multiple quantum exceptional, diabolical, and hybrid points in multimode bosonic systems: I. Inherited and genuine singularities

Kishore Thapliyal,^{1,*} Jan Peřina Jr.,^{1,†} Grzegorz Chimczak,² Anna Kowalewska-Kudłaszyk,² and Adam Miranowicz²

¹*Joint Laboratory of Optics, Faculty of Science, Palacký University,
Czech Republic, 17. listopadu 12, 771 46 Olomouc, Czech Republic*

²*Institute of Spintronics and Quantum Information, Faculty of Physics,
Adam Mickiewicz University, 61-614 Poznań, Poland*

The existence and degeneracies of quantum exceptional, diabolical, and hybrid (i.e., diabatically degenerated exceptional) singularities of simple bosonic systems composed of up to five modes with damping and/or amplification are analyzed. Their dynamics governed by quadratic non-Hermitian Hamiltonians is followed using the Heisenberg-Langevin equations. Conditions for the observation of inherited quantum hybrid points, observed directly in the dynamics of field operators, having up to third-order exceptional and second-order diabolical degeneracies are revealed. Exceptional and diabolical genuine points and their degeneracies observed in the dynamics of second-order field-operator moments are analyzed. Surprisingly, exceptional degeneracies of only second and third orders are revealed. Nevertheless the analyzed bosonic systems exhibit rich dynamics, also owing to their common second-order diabolical degeneracies.

I. INTRODUCTION

Non-Hermitian Hamiltonians had been for a long time considered not being suitable for describing real physical systems. This opinion has changed after the seminal work by Bender and Boettcher [1] who showed that the non-Hermitian Hamiltonians endowed with a parity and time symmetry (\mathcal{PT} -symmetry) exhibit real spectra in certain areas of the system parameter space. This leads to the formulation of new area of physics, i.e., non-Hermitian quantum mechanics [2–5], which has already provided numerous models [6–11] suitable for describing real quantum systems in many areas of physics. Moreover, non-Hermitian Hamiltonians exhibit new algebraic structures: It has been shown that, for certain values of parameters, there occur spectral degeneracies accompanied by degeneracies of the eigenvectors of a given Hamiltonian. Such points in a system parameter space with exceptional degeneracies (EDs) are called exceptional points (EPs) for which the dimension of the corresponding Hilbert space is reduced. This has interesting physical consequences and leads to new unexpected physical effects. It allows to enhance the precision of measurements of suitable physical quantities [12–16]. It also leads to enhanced nonlinear interactions [17, 18]. For this reason, \mathcal{PT} -symmetric systems of different kinds have been found appealing in many areas of physics including: optical waveguides [19, 20], optical lattices [21–24], spin lasers [25], optical coupled structures [26–30], coupled optical microresonators [13, 31–35], quantum-electrodynamics circuits (QED) [36], systems with complex potentials [37], optomechanical systems [38, 39], photonics molecules [40], among others. Moreover, schemes for engineering properties of EPs have

been suggested (see, e.g., [41] and references therein).

Subsequent studies have revealed also other features observed in \mathcal{PT} -symmetric systems in addition to EPs. For example, the spectral degeneracies which are not accompanied by the corresponding eigenvector degeneracies, were observed [42]. Such degeneracies do not usually lead to the above discussed physical effects and so the corresponding points in the system parameter space were named diabolical points (DPs). Note that DPs, contrary to EPs, can also be observed in Hermitian systems [42]. As pointed out in [43], it may happen that this DP or rather diabolical degeneracy (DD) occurs at an EP. In this case, ‘independent’ (i.e. with different eigenvectors) multiple spectral and eigenvector degeneracies are found in systems and we refer to them as hybrid diabolic exceptional points (HPs). Such systems then naturally exhibit a physical behavior similar to that observed at EPs. Moreover, new effects originating in diabolical degeneracy may arise. For example, the system behavior when encircling an HP has been used to construct a multi-mode optical switch [44].

Non-Hermitian \mathcal{PT} -symmetric optical bosonic systems are especially interesting from the point of view of their behavior at EPs. Their infinite-dimensional Hilbert space leads to numerous manifestations of modifications of their dynamics at quantum EPs (QEPs), i.e. EPs observed in quantum systems [18], including the effect of quantum jumps [45, 46]. The system dynamics may be followed either directly in the Hilbert space [the Liouville space of statistical operators] or in the complementary space of field-operator moments (FOMs) of all orders [47, 48]. The studies performed in the moment space of field operators in multimode bosonic systems described by non-Hermitian quadratic Hamiltonians revealed different types of degeneracies related to QEPs [43, 49]. Moreover, they allowed to sort QEPs into three classes: inherited QEPs, genuine QEPs and induced QEPs. The dynamical equations for the mean values of field operators indicated the presence of inherited QEPs and quan-

* kishore.thapliyal@upol.cz

† jan.perina.jr@upol.cz

tum HPs (QHPs) [43] that represent the core of the studied unusual behavior. The presence of such inherited QEPs and QHPs then implies the existence of genuine QEPs and QHPs [43] observed in the dynamics of higher-order FOMs. With the increasing FOM order, the degeneracies of genuine QEPs and QHPs increase. Moreover, similar or identical FOMs, as being related by the field commutation relations, arise in the formal construction of higher-order FOMs. Thus, we can also define induced QEPs and QHPs [43] that further enlarge the multiplicity of the spectral degeneracies. However, as these redundant FOMs share their time evolution with the FOMs contributing to genuine QEPs and QHPs, they do not lead to additional diversity of the system evolution. Thus, they are not interesting from the point of view of the dynamics of FOMs of a given order. Thus, this dynamics is fully characterized by the corresponding genuine QEPs and QHPs. As the properties of genuine QEPs and QHPs originate in those of the inherited QEPs and QHPs, the analysis of the latter is crucial for the understanding of a system evolution. For this reason, it is important to identify the inherited QEPs and QHPs and their degeneracies in simple bosonic systems formed by smaller numbers of bosonic modes. This analysis may then be exploited for further studies of physical effects in such systems.

The system composed of two mutually interacting modes, one being damped and the other amplified, was already analyzed from this point of view in Ref. [43]. This analysis may be considered as the simplest building block useful for investigations of more complex bosonic systems. Here, we consider systems composed of up to five modes in different configurations promising for the observation of QEPs and QHPs. Looking for inherited QEPs with higher-order EDs is the main goal of our investigations. It is motivated by the fact that the higher is the ED order, the more modified is the system dynamics at a QEP. This then enhances the physical effects specific to QEPs like improvement in measurement precision or enhancement of nonlinear effects.

As we have been able to reveal only up to the third-order ED of QEPs of the analyzed systems, we continue our analysis in Ref. [50], being the second part of this paper, in which we pay attention to the spectral degeneracies of non-Hermitian Hamiltonians observed only in specific subspaces of the systems' Liouville spaces as well as non-Hermitian Hamiltonians with unidirectional coupling. In Ref. [50], we also address numerical identification of QEPs and QHPs. Moreover, we extend the analysis of the genuine and induced QEPs and QHPs by considering the FOMs of a general order.

The paper is organized as follows. A two-mode bosonic system with unequal damping and/or amplification rates, as the simplest considered model, is analyzed in Sec. II. Section III brings the analysis of a related three-mode linear system. The corresponding generalized four-mode linear and circular systems are investigated in Sec. IV whereas the analysis of the five-mode linear and pyramid

systems is found in Sec. V. Section VI brings conclusions.

II. TWO-MODE BOSONIC SYSTEM: BASIC BUILDING BLOCKS

We begin with the consideration of one of the simplest \mathcal{PT} -symmetric bosonic systems that is composed of two modes: one being attenuated and the other amplified [for the scheme, see Fig. 1(a)]. We note that even a one-mode bosonic system may exhibit \mathcal{PT} -symmetric behavior, as shown in Ref. [51]. We also pay attention only to the systems described by quadratic Hamiltonians that lead to linear exactly-solvable Heisenberg equations. Though these Hamiltonians lead to linear dynamical equations, they allow for describing the nonlinear effect of photon-pair generation and annihilation. This effect is commonly used in various quantum optical systems to generate entangled [52] and squeezed [53, 54] states of light. \mathcal{PT} -symmetry restricts the form of the studied non-Hermitian Hamiltonian such that the underlying dynamics is described by the dynamical matrix composed of typical 2×2 submatrices. They are also used to build the matrices of more complex \mathcal{PT} -symmetric bosonic systems. Moreover, we also consider bosonic systems in which damping and amplification are not in balance, which is a typical situation of \mathcal{PT} -symmetric systems. In this unbalanced case, relying on the results presented in Ref. [55], we may introduce a specific interaction picture in which the average damping or amplification dynamics is projected out and the remaining dynamics exhibits the features found in \mathcal{PT} -symmetric systems.

Under these conditions, we may write the quadratic Hamiltonian of the considered two-mode bosonic system in the interaction picture as follows:

$$\hat{H}_2 = \left[\hbar \epsilon \hat{a}_1^\dagger \hat{a}_2 + \hbar \kappa \hat{a}_1 \hat{a}_2 \right] + \text{H.c.}, \quad (1)$$

where \hat{a}_j (\hat{a}_j^\dagger) stands for the annihilation (creation) operator of the j th mode, $j = 1, 2$, ϵ is the linear coupling strength between the modes, and κ is the nonlinear coupling strength between the modes. Symbol H.c. replaces the Hermitian-conjugated terms. Whereas the linear coupling originates in the spatial overlap of the mode electric-field amplitudes, the nonlinear coupling arises in the three-mode parametric process with strong pumping [56]. The damping (amplification) of modes occurs as a consequence of the interaction with the reservoir whose two-level atoms are in the ground (excited) state [43]. Projecting out the reservoir two-level atoms, we are left with the damping (amplification) rate γ_j of j th damped (amplified) mode and the corresponding Langevin stochastic operator forces, \hat{L}_j and \hat{L}_j^\dagger , in the dynamical Heisenberg-Langevin equations. We note that properties of the Langevin operator forces differ for the damping and amplification processes and they have to be chosen such that the field-operator commutation

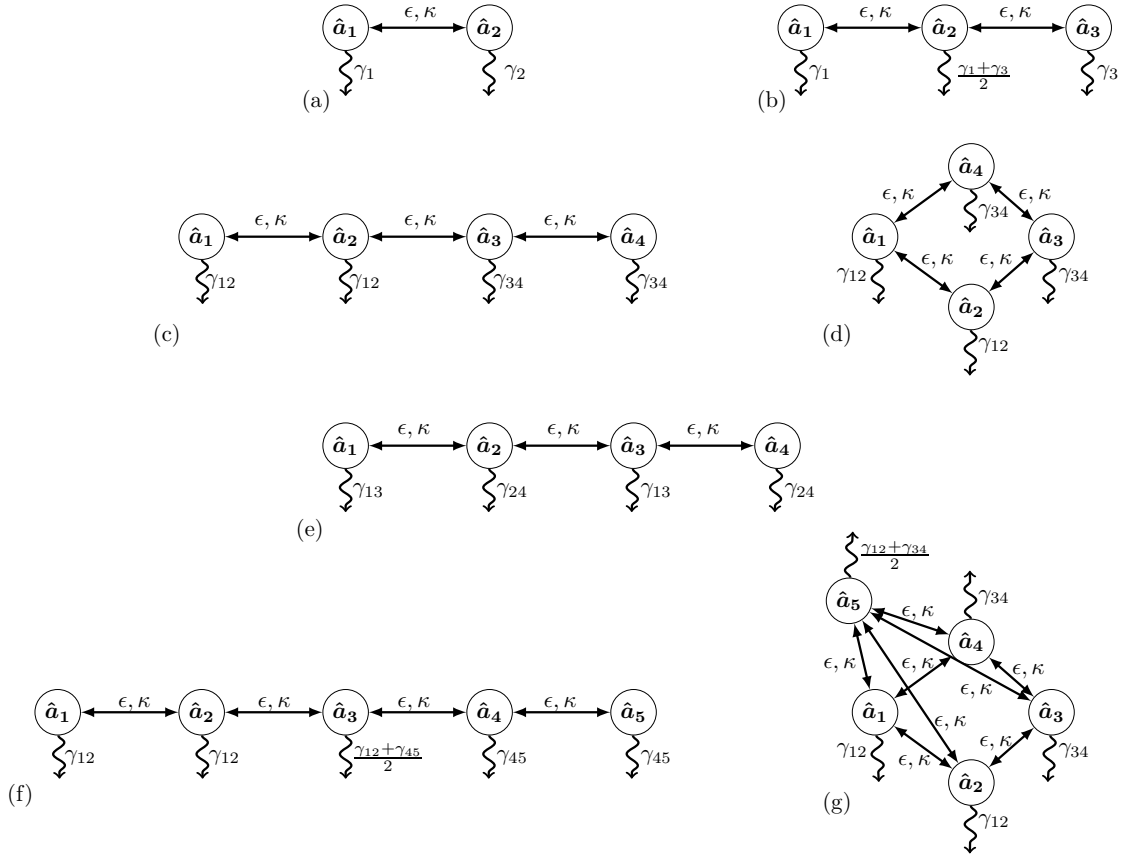


FIG. 1. Schematic diagrams of the bosonic systems composed of (a) two, (b) three, (c–e) four, and (f,g) five modes with typical linear, circular, and pyramid configurations that exhibit QHPs. Strengths ϵ and κ characterize, respectively, the linear and nonlinear coupling between the modes, γ , with subscripts indicating the mode number(s), are the damping or amplification rates, and annihilation operators \hat{a} identify the mode number via their subscripts, and γ_{jk} indicates that $\gamma_j = \gamma_k$.

relations are fulfilled. This results in the corresponding fluctuation-dissipation theorems [47, 57] formulated within the Heisenberg-Langevin formalism.

Using the two-mode Hamiltonian in Eq. (1), we derive the Heisenberg-Langevin equations written for the vector $\hat{\mathbf{a}} = [\hat{a}_1, \hat{a}_2]^T \equiv [\hat{a}_1, \hat{a}_1^\dagger, \hat{a}_2, \hat{a}_2^\dagger]^T$ of field operators and vector $\hat{\mathbf{L}} = [\hat{L}_1, \hat{L}_1^\dagger, \hat{L}_2, \hat{L}_2^\dagger]^T$ of the Langevin operator forces as follows [58]:

$$\frac{d\hat{\mathbf{a}}}{dt} = -i\mathbf{M}^{(2)}\hat{\mathbf{a}} + \hat{\mathbf{L}}. \quad (2)$$

In Eq. (2), the dynamical matrix $\mathbf{M}^{(2)}$,

$$\mathbf{M}^{(2)} = \begin{bmatrix} -i\tilde{\gamma}_1 & \boldsymbol{\xi} \\ \boldsymbol{\xi} & -i\tilde{\gamma}_2 \end{bmatrix}, \quad (3)$$

is expressed in terms of 2×2 submatrices $\tilde{\gamma}_j$, $j = 1, 2$, and $\boldsymbol{\xi}$ defined as:

$$\tilde{\gamma}_j = \begin{bmatrix} \gamma_j/2 & 0 \\ 0 & \gamma_j/2 \end{bmatrix}, \quad \boldsymbol{\xi} = \begin{bmatrix} \epsilon & \kappa \\ -\kappa & -\epsilon \end{bmatrix}, \quad (4)$$

where γ_j is the damping or amplification rate of the mode j that is accompanied by the corresponding Langevin operator forces.

The 2×2 matrices, $\tilde{\gamma}_j$ ($j = 1, 2$) and $\boldsymbol{\xi}$, given in Eq. (4) can be simultaneously diagonalized using the diagonalization transformation appropriate to the matrix $\boldsymbol{\xi}$ as the remaining two matrices are linearly proportional to the unity matrix and, thus, are not modified by the transformation. This diagonalization transformation then factorizes (decomposes) the matrix $\mathbf{M}^{(2)}$ in Eq. (3) into two independent 2×2 matrices with the structure of the original matrix $\mathbf{M}^{(2)}$.

Denoting an eigenvalue of the matrix $\boldsymbol{\xi}$ as ξ , we may express the eigenfrequencies $\lambda_{1,2}^{M^{(2)}}$ and eigenvectors $\mathbf{y}_{1,2}^{M^{(2)}}$ of the factorizing (decomposing) 2×2 matrices of the matrix $\mathbf{M}^{(2)}$ in Eq. (2) in the following common form:

$$\lambda_{1,2}^{M^{(2)}} = -i\gamma_{\pm} \mp \beta \quad (5)$$

and

$$\mathbf{y}_{1,2}^{M^{(2)}} = \left[-\frac{i\gamma_{\pm} \pm \beta}{\xi}, 1 \right]^T, \quad (6)$$

where $4\gamma_{\pm} = \gamma_1 \pm \gamma_2$ and $\beta^2 = \xi^2 - \gamma_-^2$.

The eigenvalues $\lambda_{1,2}^\xi$ and the corresponding eigenvectors $\mathbf{y}_{1,2}^\xi$ of the matrix $\boldsymbol{\xi}$ are simply derived in the form:

$$\lambda_{1,2}^\xi = \mp \zeta \quad (7)$$

and

$$\mathbf{y}_{1,2}^\xi = \left[-\frac{\epsilon \mp \zeta}{\kappa}, 1 \right]^T, \quad (8)$$

where $\zeta = \sqrt{\epsilon^2 - \kappa^2}$.

Combing the above two results for the matrix diagonalization, we can express the eigenvalues $\Lambda^{M(2)}$ of the 4×4 matrix $\mathbf{M}^{(2)}$ in Eq. (2) as $\Lambda_{1,3}^{M(2)} = \lambda_{1,2}^{M(2)}$ for $\xi = \lambda_1^\xi$ and $\Lambda_{2,4}^{M(2)} = \lambda_{1,2}^{M(2)}$ for $\xi = \lambda_2^\xi$, i.e.:

$$\begin{aligned} \Lambda_1^{M(2)} &= \Lambda_2^{M(2)} = -i\gamma_+ - \beta, \\ \Lambda_3^{M(2)} &= \Lambda_4^{M(2)} = -i\gamma_+ + \beta, \end{aligned} \quad (9)$$

and $\beta = \sqrt{\zeta^2 - \gamma_-^2}$. We note that the average damping or amplification rate $\gamma_+ = 0$ in the usual \mathcal{PT} -symmetric systems.

Similarly as the eigenvalues, we obtain the eigenvectors along the formulas

$$\begin{aligned} \mathbf{Y}_j^{M(2)} &= \left[y_{1,1}^{M(2)}(\xi = \lambda_j^\xi) \mathbf{y}_j^\xi, y_{1,2}^{M(2)}(\xi = \lambda_j^\xi) \mathbf{y}_j^\xi \right]^T, \\ &\quad \text{for } j = 1, 2, \\ \mathbf{Y}_j^{M(2)} &= \left[y_{2,1}^{M(2)}(\xi = \lambda_{j-2}^\xi) \mathbf{y}_{j-2}^\xi, y_{2,2}^{M(2)}(\xi = \lambda_{j-2}^\xi) \mathbf{y}_{j-2}^\xi \right]^T, \\ &\quad \text{for } j = 3, 4, \end{aligned} \quad (10)$$

in the form:

$$\begin{aligned} \mathbf{Y}_{1,2}^{M(2)} &= \left[\frac{(\mp\epsilon + \zeta)\chi}{\kappa\zeta}, \pm\frac{\chi}{\zeta}, -\frac{(\epsilon \mp \zeta)}{\kappa}, 1 \right]^T, \\ \mathbf{Y}_{3,4}^{M(2)} &= \left[\frac{(\pm\epsilon - \zeta)\chi^*}{\kappa\zeta}, \mp\frac{\chi^*}{\zeta}, -\frac{(\epsilon \mp \zeta)}{\kappa}, 1 \right]^T, \end{aligned} \quad (11)$$

where $\chi = i\gamma_- + \beta$.

The formula in Eq. (9) provides the two pairs of coinciding eigenvalues. However, Eq. (11) for the corresponding eigenvectors reveal no eigenvector degeneracy in general. On the other hand, χ is purely imaginary for $\beta = 0$, which leads to $\mathbf{Y}_1^{M(2)} = \mathbf{Y}_3^{M(2)}$ and $\mathbf{Y}_2^{M(2)} = \mathbf{Y}_4^{M(2)}$, while having all the eigenvalues the same. So we observe the second-order degeneration in the Hilbert space that is formed by two second-order QEPs with identical eigenvalues. We, thus, have a QHP with second-order DD and ED in this case. The condition $\beta = 0$ implies that the eigenvalues and eigenvectors of the 2×2 matrix $\mathbf{M}^{(2)}$ given in Eqs. (5) and (6) coincide. The second-order ED, thus, originates in the 2×2 form of matrix $\mathbf{M}^{(2)}$. We note that this degeneracy can be verified by transforming the matrix $\mathbf{M}^{(2)}$ for $\beta = 0$ into its Jordan form

$$\mathbf{J}_{\mathbf{M}^{(2)}} = \begin{bmatrix} -i\gamma_+ & 1 \\ 0 & -i\gamma_+ \end{bmatrix}. \quad (12)$$

On the other hand, the eigenvalues of 2×2 submatrix $\boldsymbol{\xi}$ written in Eq. (7) point out at the origin of DD: They differ just by the sign, but they lead to the same value of β , i.e., to the same eigenvalue $\lambda_{1,2}^{M(2)}$ of the 2×2 matrix $\mathbf{M}^{(2)}$. DD is then implied by the fact that the eigenvectors $\mathbf{y}_{1,2}^\xi$ of 2×2 submatrix $\boldsymbol{\xi}$ in Eq. (8) differ for $\zeta \neq 0$.

These findings about the structure of the matrices describing the dynamical equations have their counterpart in the structure of the analyzed two-mode \mathcal{PT} -symmetric system. The 2×2 matrix $\boldsymbol{\xi}$, defined in Eq. (4), connects pairs of the annihilation and creation operators of different modes. As such it forms the basic building block of more complex \mathcal{PT} -symmetric systems, together with the damping and/or amplification matrices $\tilde{\gamma}_j$ in Eq. (4). In more complex \mathcal{PT} -symmetric systems, the dependencies of the eigenvalues of the dynamical matrices $\mathbf{M}^{(n)}$ ($n = 2, 3, \dots$) on the eigenvalues $\lambda_{1,2}^\xi$ of the $\boldsymbol{\xi}$ matrix are typically quadratic. This, thus, results in the observation of second-order DD in the dynamical features of the matrices $\mathbf{M}^{(n)}$. In this case, the eigenvalue analysis of the considered systems considerably simplifies and we may restrict our attention to only the $n \times n$ matrices $\mathbf{M}^{(n)}$, when a detailed eigenvalue analysis is performed.

The condition $\beta = 0$ for observing QHPs can be analyzed in the space of system parameters $(\epsilon, \kappa, \gamma_1, \gamma_2)$ as follows. The quadratic Hamiltonian $\hat{H}^{(2)}$ in Eq. (1) provides the linear Heisenberg-Langevin equations that allow for the temporal rescaling ϵt , i.e., only the relative parameters $(\kappa/\epsilon, \gamma_1/\epsilon, \gamma_2/\epsilon)$ suffice in characterizing the system dynamics. Moreover, the structure of the analyzed systems is such that the average damping or amplification rates γ_+ influences equally only the eigenvalues, but it does not modify the eigenvectors. This makes the space of the system parameters effectively two-dimensional with the spanning parameters $(\kappa/\epsilon, \gamma_-/\epsilon)$. Using these parameters, the condition $\beta = 0$ is expressed as follows:

$$\frac{\kappa^2}{\epsilon^2} + \frac{\gamma_-^2}{\epsilon^2} = 1. \quad (13)$$

Thus, the QHPs form a circle with the unit radius in the space $(\kappa/\epsilon, \gamma_-/\epsilon)$, as shown in Fig. 1. We note that, at this circle, there is a specific point at $\gamma_- = 0$ in which all four eigenvectors, given in Eq. (10), are the same which gives raise to the fourth-order QEP. However, this corresponds to the system in which both modes are equally damped or amplified. It is worth noting that the eigenvectors of both matrices $\mathbf{M}^{(2)}$, given in Eq. (3), and $\boldsymbol{\xi}$, in Eq. (4), are degenerated at this point.

Deeper insight into the structure of higher-order FOMs, as well as the system dynamics, can be obtained once we transform the Heisenberg-Langevin equations (2) into the form in which the dynamical matrix has the diagonal form. Using the transformation matrix $\mathbf{P} = [\mathbf{Y}_1^{M(2)}, \mathbf{Y}_2^{M(2)}, \mathbf{Y}_3^{M(2)}, \mathbf{Y}_4^{M(2)}]$ formed from the eigenvectors in Eq. (10), we define the corresponding

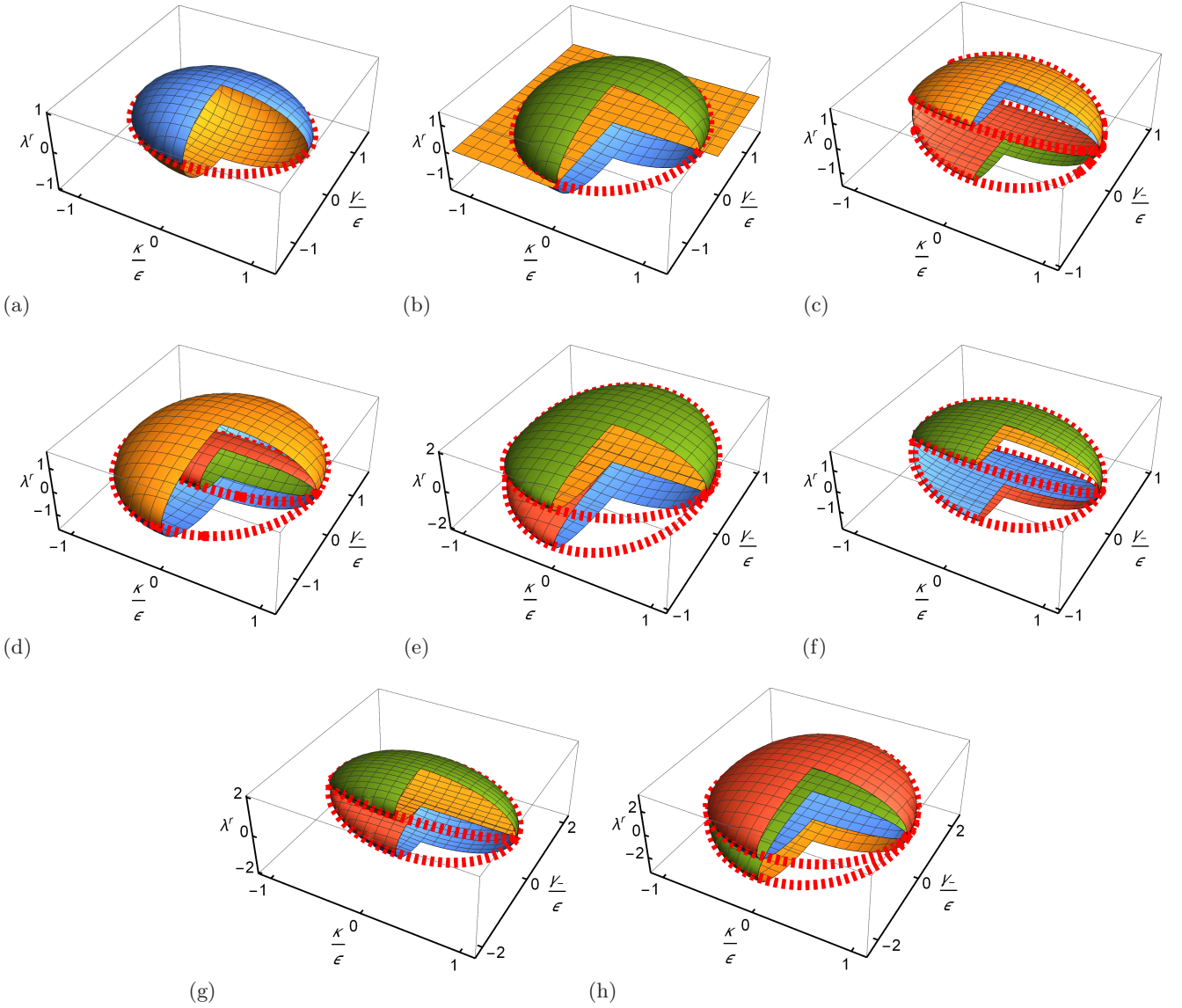


FIG. 2. Real parts λ^r of the eigenvalues (a) $\lambda_{1,2}^{M^{(2)}}$ of the matrix $\mathbf{M}^{(2)}$, given in Eq. (9), for the two-mode bosonic system, (b) $\lambda_{1,2,3}^{M^{(3)}}$ of the matrix $\mathbf{M}^{(3)}$, given in Eq. (23), for the three-mode linear bosonic system, (c) [(d)] $\lambda_{1,\dots,4}^{M_{11}^{(4)}} [\lambda_{1,\dots,4}^{M_{12}^{(4)}}]$ of the matrix $\mathbf{M}_{11}^{(4)} [\mathbf{M}_{12}^{(4)}]$, given in Eqs. (28), (29), and [(33)] for the four-mode linear bosonic system with neighbor modes having equal [different] damping and/or amplification rates, (e) $\lambda_{1,\dots,4}^{M_{c1}^{(4)}}$ of the matrix $\mathbf{M}_{c1}^{(4)}$, given in Eq. (38), for the four-mode circular bosonic system with neighbor modes having equal the damping and/or amplification rates, (f) $\lambda_{2,\dots,5}^{M_1^{(5)}}$ of the matrix $\mathbf{M}_1^{(5)}$, given by Eq. (44), for the five-mode linear bosonic system, and (g,h) $\lambda_{2,\dots,5}^{M_p^{(5)}}$ of the matrix $\mathbf{M}_p^{(5)}$, given in Eq. (51), for the five-mode pyramid bosonic system assuming (g) $\beta_1 = 0$ and (h) $\beta_2 = 0$. The eigenvalues are drawn in the parameter space $(\kappa/\epsilon, \gamma_-/\epsilon)$, where ϵ (κ) is the linear (nonlinear) coupling strength and γ_- the difference of the damping/amplification rates in individual models. Dashed red curves indicate the positions of the QHPs given by (a,e,g) Eq. (13), (b) Eq. (25), (c) Eq. (32), (d) Eq. (36), (f) Eq. (49), and (h) Eq. (56).

field operators $\hat{\mathbf{b}} = [\hat{b}_1, \hat{b}_2, \hat{b}_1^\dagger, \hat{b}_2^\dagger]^T$, the Langevin operator forces $\hat{\mathbf{K}} = [\hat{K}_1, \hat{K}_2, \hat{K}_1^\dagger, \hat{K}_2^\dagger]^T$, and the diagonal dynamical matrix $\mathbf{\Lambda}^{(2)}$:

$$\mathbf{\Lambda}^{(2)} = \mathbf{P}^{-1} \mathbf{M}^{(2)} \mathbf{P}, \quad \hat{\mathbf{b}} = \mathbf{P}^{-1} \hat{\mathbf{a}}, \quad \hat{\mathbf{K}} = \mathbf{P}^{-1} \hat{\mathbf{L}}. \quad (14)$$

We note that the order of elements in the operator vector $\hat{\mathbf{b}}$ (and similarly in the vector $\hat{\mathbf{K}}$ of the accompanying Langevin operator forces) is given by the numbering of the eigenvalues in Eq. (9) and the corresponding diagonalization transform.

In the transformed basis, the Heisenberg-Langevin

equations take the form:

$$\frac{d\hat{\mathbf{b}}}{dt} = -i\mathbf{\Lambda}^{(2)}\hat{\mathbf{b}} + \hat{\mathbf{K}}. \quad (15)$$

We note that the positions of the newly-defined annihilation and creation operators in the vector $\hat{\mathbf{b}}$, as well as the positions of the accompanying Langevin operator forces in the vector $\hat{\mathbf{K}}$, differ from those in the original vectors $\hat{\mathbf{a}}$ and $\hat{\mathbf{L}}$ defined above Eq. (2). The solution to Eq. (15) is expressed as:

$$\begin{aligned} \hat{\mathbf{b}}(t) &= \exp(-i\mathbf{\Lambda}^{(2)}t)\hat{\mathbf{b}}(0) \\ &+ \int_0^t dt' \exp[-i\mathbf{\Lambda}^{(2)}(t-t')]\hat{\mathbf{K}}(t'). \end{aligned} \quad (16)$$

Using the inverse transformation, we arrive at the solution for the operators $\hat{\mathbf{a}}$, which reads:

$$\begin{aligned} \hat{\mathbf{a}}(t) &= \mathbf{P} \exp(-i\mathbf{\Lambda}^{(2)}t) \mathbf{P}^{-1} \hat{\mathbf{a}}(0) \\ &+ \int_0^t dt' \mathbf{P} \exp[-i\mathbf{\Lambda}^{(2)}(t-t')] \mathbf{P}^{-1} \hat{\mathbf{L}}(t'). \end{aligned} \quad (17)$$

The solution in Eq. (17) of the Heisenberg-Langevin equations in the diagonal form together with the assumption of the Gaussian Markovian character of the Langevin operator forces allows us to follow the dynamics of FOMs of an arbitrary order. We note that, from the point of view of eigenfrequencies, the FOMs of a given order form a closed dynamical system [43]. In this dynamics, we observe the genuine QEPs and QHPs that are derived from the inherited QEPs and QHPs discussed above. In general, the higher is the FOM order, the higher are the observed EDs and DDs at QEPs and QHPs. These degeneracies were systematically studied in Ref. [43] up to the fourth-order FOMs. Here, we summarize in Tab. I these degeneracies for up to second-order FOMs to give the comparison of the QEP and QHP degeneracies found in the first- and second-order FOM dynamics. It is useful to compare QEP and QHP degeneracies in Tab. I with those observed in the systems with greater numbers of modes presented below.

We note that the quadratic form of Hamiltonian \hat{H}_2 , in Eq. (1), is not the most general one. It can be extended by considering additional terms describing local squeezing in modes 1 and 2 described by a constant g , as it was done in Ref. [43]:

$$\hat{H}_2 = \left[\hbar\epsilon\hat{a}_1^\dagger\hat{a}_2 + \hbar\kappa\hat{a}_1\hat{a}_2 + \sum_{j=1,2} \hbar g\hat{a}_j^{\dagger 2}/2 \right] + \text{H.c.} \quad (18)$$

However, the structure of the dynamical matrix $\mathbf{M}^{(2)}$, built from the 2×2 submatrices, is broken for nonzero values of the constant g . This results in the loss of the second-order DD that follows from the structure of the ξ and $\tilde{\gamma}_j$ matrices written in Eq. (4). As a consequence, only second-order inherited QEPs occur for $g \neq 0$ in the parameter space $(\kappa/\epsilon, \gamma_-/\epsilon, g/\epsilon)$. Detailed analysis

of the positions of inherited QEPs, as well as EDs and DDs of QEPs and QHPs observed in the FOMs dynamics was provided in Ref. [43]. Similar reduction of eigenvalue and eigenvector degeneracies in the Hilbert space after including these terms was observed in more complex bosonic systems. We further pay attention only to the systems described by quadratic Hamiltonians without these terms.

III. THREE-MODE BOSONIC SYSTEM

The above-analyzed two-mode system provided QHPs with second-order ED and DD. Whereas the DD originates in the mutual coupling between the two modes (described by the strengths ϵ and κ), the ED arises from different strengths of damping and amplification of the modes and a given system configuration. Bosonic systems composed of more than two modes give a promise for revealing QHPs with a larger number of EDs and DDs. However, the question is how to choose a suitable configuration of interactions among the modes and their damping and/or amplification rates. Whereas the parity symmetry is useful in seeking promising geometries, the temporal symmetry allows to define suitable relations among the damping and amplification rates. In this section, we begin our investigation by considering three-mode bosonic systems in the linear configuration, and define specific conditions under which QHPs occur. In the following sections, we extend our analysis to the four- and five-mode systems. The geometries together with their characteristic parameters are schematically shown in Fig. 1. We also identify the positions of QHPs in the corresponding parameter spaces. Moreover, we analyze the occurrence of genuine QEPs and QHPs and determine their EDs and DDs from the point of view of the dynamics of second-order FOMs.

Among the bosonic systems with three modes we succeeded in identifying QHPs in the linear configuration that is shown in Fig. 1(b). Similar system in this configuration was experimentally realized in Ref. [59]. We note that a QEP with third-order ED was identified in Ref. [60] in an optomechanical system of three interacting bosonic modes. Hamiltonian \hat{H}_3 of such a system can be written as follows:

$$\hat{H}_3 = \left[\hbar\epsilon\hat{a}_1^\dagger\hat{a}_2 + \hbar\epsilon\hat{a}_2^\dagger\hat{a}_3 + \hbar\kappa\hat{a}_1\hat{a}_2 + \hbar\kappa\hat{a}_2\hat{a}_3 \right] + \text{H.c.} \quad (19)$$

Using the 2×2 submatrices $\tilde{\gamma}_j$, $j = 1, 2, 3$, describing mode damping or amplification, and ξ defined in Eq. (4), we derive the Heisenberg-Langevin equations in the form

$$\frac{d\hat{\mathbf{a}}}{dt} = -i\mathbf{M}^{(3)}\hat{\mathbf{a}} + \hat{\mathbf{L}}, \quad (20)$$

Λ_j^i	Λ_j^r	Moments		Moment deg.	Genuine and induced QHPs		Genuine QHPs	
					Partial QDP x QEP deg.	Partial QDP x QEP deg.	Partial QDP x QEP deg.	Partial QDP x QEP deg.
γ_+	$\mp\beta$	$\langle \hat{b}_1 \rangle, \langle \hat{b}_1^\dagger \rangle$	$\langle \hat{\mathbf{B}}_1 \rangle$	1	1x2	2x2	1x2	2x2
		$\langle \hat{b}_2 \rangle, \langle \hat{b}_2^\dagger \rangle$	$\langle \hat{\mathbf{B}}_2 \rangle$	1	1x2		1x2	
$2\gamma_+$	$\mp 2\beta$	$\langle \hat{b}_1 \hat{b}_2 \rangle, \langle \hat{b}_1^\dagger \hat{b}_2^\dagger \rangle$	$\langle \hat{\mathbf{B}}_1 \hat{\mathbf{B}}_2 \rangle$	2	2x4	4x4	1x4	1x4 +
	$\beta - \beta$	$\langle \hat{b}_1^\dagger \hat{b}_2 \rangle$		2				
	$\beta - \beta$	$\langle \hat{b}_1 \hat{b}_2^\dagger \rangle$		2				
	$\mp 2\beta$	$\langle \hat{b}_1^2 \rangle, \langle \hat{b}_1^{\dagger 2} \rangle$	$\langle \hat{\mathbf{B}}_1^2 \rangle$	1	1x4		1x3	2x3
	$\beta - \beta$	$\langle \hat{b}_1^\dagger \hat{b}_1 \rangle$		2				
	$\mp 2\beta$	$\langle \hat{b}_2^2 \rangle, \langle \hat{b}_2^{\dagger 2} \rangle$	$\langle \hat{\mathbf{B}}_2^2 \rangle$	1	1x4		1x3	
	$\beta - \beta$	$\langle \hat{b}_2^\dagger \hat{b}_2 \rangle$		2				

TABLE I. Real and imaginary parts of the complex eigenfrequencies $\Lambda_j^r - i\Lambda_j^i$ of the matrix $\mathbf{M}^{(2)}$ given in Eq. (3) for the two-mode bosonic system derived from the equations for the FOMs up to second order. The corresponding moments in the ‘diagonalized’ field operators are written together with their degeneracies (deg.) coming from different positions of the field operators. The DDs of QHPs (partial DDs) derived from the indicated FOMs and the EDs of the constituting QEPs are given. Both genuine and induced QEPs and QHPs are considered. The operators $\hat{\mathbf{B}}_j$ for $j = 1, 2$ are defined in the lines written for $\Lambda_j^i = \gamma_+$ devoted to the first-order FOMs.

where

$$\mathbf{M}^{(3)} = \begin{bmatrix} -i\tilde{\gamma}_1 & \xi & \mathbf{0} \\ \xi & -i\tilde{\gamma}_2 & \xi \\ \mathbf{0} & \xi & -i\tilde{\gamma}_3 \end{bmatrix}, \quad (21)$$

and $\mathbf{0}$ denotes the 2×2 null matrix, while $\hat{\mathbf{a}} = [\hat{\mathbf{a}}_1, \hat{\mathbf{a}}_2, \hat{\mathbf{a}}_3]^T \equiv [\hat{a}_1, \hat{a}_1^\dagger, \hat{a}_2, \hat{a}_2^\dagger, \hat{a}_3, \hat{a}_3^\dagger]^T$ and $\hat{\mathbf{L}} = [\hat{L}_1, \hat{L}_1^\dagger, \hat{L}_2, \hat{L}_2^\dagger, \hat{L}_3, \hat{L}_3^\dagger]^T$.

Assuming the condition

$$2\gamma_2 = \gamma_1 + \gamma_3, \quad (22)$$

the eigenvalues $\lambda_j^{M^{(3)}}$ ($j = 1, 2, 3$) of the dynamical matrix $\mathbf{M}^{(3)}$ in Eq. (21) share the common damping or amplification rate γ_+ and we may write

$$\lambda_1^{M^{(3)}} = -i\gamma_+, \quad \lambda_{2,3}^{M^{(3)}} = -i\gamma_+ \mp \beta, \quad (23)$$

using $4\gamma_\pm = \gamma_1 \pm \gamma_3$ and $\beta^2 = 2\xi^2 - \gamma_-^2$; ξ being an eigenvalue of the matrix ξ in Eq. (4). The eigenvectors corresponding to the eigenvalues $\lambda_j^{M^{(3)}}$ in Eq. (23) are derived in the form:

$$\mathbf{y}_1^{M^{(3)}} = \left[-1, -\frac{i\gamma_-}{\xi}, 1 \right]^T, \\ \mathbf{y}_{2,3}^{M^{(3)}} = \left[1 + \frac{i\gamma_-(i\gamma_- \pm \beta)}{\xi^2}, -\frac{i\gamma_- \pm \beta}{\xi}, 1 \right]^T. \quad (24)$$

Provided that $\beta = 0$, the three eigenvalues $\lambda_j^{M^{(3)}}$ for $j = 1, 2, 3$ in Eq. (23), as well as the corresponding eigenvectors in Eq. (24), are equal and, thus, third-order QEPs of the 3×3 matrix $\mathbf{M}^{(3)}$ are found. Taking into account the structure of the submatrices of the matrix $\mathbf{M}^{(3)}$, these QEPs are in fact QHPs with second-order DD. Substituting for the eigenvalues ξ of matrix ξ from Eq. (7),

the condition $\beta = \sqrt{2\xi^2 - \gamma_-^2} = 0$ for having a QHP attains the form:

$$\frac{\kappa^2}{\epsilon^2} + \frac{\gamma_-^2}{2\epsilon^2} = 1. \quad (25)$$

This condition is visualized by the red dashed curve in Fig. 2(b) that shows the real parts of the eigenvalues $\lambda_j^{M^{(3)}}$ as they vary in the parameter space ($\kappa/\epsilon, \gamma_-/\epsilon$).

The analysis of QEPs and QHPs appropriate for the FOM dynamics requires the construction of eigenvalues and eigenvectors of the matrix $\mathbf{M}^{(3)}$ in its full 6×6 space combining the eigenvalues and eigenvectors in Eqs. (24) and (25) with those of the matrix ξ given in Eqs. (7) and (8). They are written in Appendix A. The obtained eigenvectors then allow us to introduce new field operators $\hat{\mathbf{b}} = [\hat{b}_1, \hat{b}_1^\dagger, \hat{b}_2, \hat{b}_3, \hat{b}_2^\dagger, \hat{b}_3^\dagger]^T$ in which the dynamical matrix $\mathbf{M}^{(3)}$ of the Heisenberg-Langevin equations attains its diagonal form $\Lambda^{(3)}$, similarly as it was done in Sec. II in the case of the two-mode system. The QEPs and QHPs predicted in the dynamics of the first- and second-order FOMs are summarized in Tab. II.

IV. FOUR-MODE BOSONIC SYSTEMS

Let us move to the investigations of four-mode bosonic systems, in which we revealed QEPs and QHPs in two arrangements: linear and circular. In the linear arrangement, we consider two configurations that differ by the damping and/or amplification rates assigned to the modes: Either the neighbor modes share their damping and/or amplification rates or their rates differ. On the other hand, equal damping and/or amplification rates of the neighbor modes are needed in the circular arrangement to reveal QEPs and QHPs.

Λ_j^i	Λ_j^r	Moments	Moment deg.	Genuine and induced QHPs		Genuine QHPs	
				Partial QDP x QEP deg.	Partial QDP x QEP deg.	Partial QDP x QEP deg.	Partial QDP x QEP deg.
γ_+	$0, \mp\beta$	$\langle b_1 \rangle, \langle b_2 \rangle, \langle b_3^\dagger \rangle$	$\langle \tilde{B}_1 \rangle$	1	1x3	2x3	1x3
	$0, \mp\beta$	$\langle b_1^\dagger \rangle, \langle b_3 \rangle, \langle b_3^\dagger \rangle$	$\langle \tilde{B}_2 \rangle$	1	1x3	1x3	2x3
$2\gamma_+$	0	$\langle b_1^2 \rangle$	$\langle \tilde{B}_1^2 \rangle$	1	1x9	4x9	1x6
	$\mp\beta$	$\langle b_1 b_2 \rangle, \langle b_1 b_2^\dagger \rangle$		2			2x6 +
	$\mp 2\beta$	$\langle b_2^2 \rangle, \langle b_2^{\dagger 2} \rangle$		1			
	$\beta - \beta$	$\langle b_2^\dagger b_2 \rangle$		2			
	0	$\langle b_1^\dagger b_1 \rangle$	$\langle \tilde{B}_2 \tilde{B}_1 \rangle$	2	2x9		1x9
	$\mp\beta$	$\langle b_1^\dagger b_2 \rangle, \langle b_1^\dagger b_2^\dagger \rangle$		2		1x9	
	$\mp\beta$	$\langle b_3 b_1 \rangle, \langle b_3^\dagger b_1 \rangle$		2			
	$\mp 2\beta$	$\langle b_3 b_2 \rangle, \langle b_3^\dagger b_2^\dagger \rangle$		2			
	$\beta - \beta$	$\langle b_3 b_2^\dagger \rangle, \langle b_3^\dagger b_2 \rangle$		2			
	0	$\langle b_1^{\dagger 2} \rangle$	$\langle \tilde{B}_2^2 \rangle$	1	1x9		1x6
	$\mp\beta$	$\langle b_1^\dagger b_3 \rangle, \langle b_1^\dagger b_3^\dagger \rangle$		2			
	$\mp 2\beta$	$\langle b_3^2 \rangle, \langle b_3^{\dagger 3} \rangle$		1			
	$\beta - \beta$	$\langle b_3^\dagger b_3 \rangle$		2			

TABLE II. Real and imaginary parts of the complex eigenfrequencies $\Lambda_j^r - i\Lambda_j^i$ of the matrix $\mathbf{M}^{(3)}$, given in Eq. (21), for the linear three-mode bosonic system derived from the equations for the FOMs up to second order. For details, see the caption to Tab. I.

A. Linear configurations

In the linear configuration, the quadratic Hamiltonian $\hat{H}_{4,1}$ of four-mode system is expressed in the form

$$\begin{aligned} \hat{H}_{4,1} = & \left[\hbar\epsilon\hat{a}_1^\dagger\hat{a}_2 + \hbar\epsilon\hat{a}_2^\dagger\hat{a}_3 + \hbar\epsilon\hat{a}_3^\dagger\hat{a}_4 + \hbar\kappa\hat{a}_1\hat{a}_2 \right. \\ & \left. + \hbar\kappa\hat{a}_2\hat{a}_3 + \hbar\kappa\hat{a}_3\hat{a}_4 \right] + \text{H.c.} \end{aligned} \quad (26)$$

The corresponding Heisenberg-Langevin equations are derived as follows:

$$\frac{d\hat{\mathbf{a}}}{dt} = -i\mathbf{M}_1^{(4)}\hat{\mathbf{a}} + \hat{\mathbf{L}}, \quad (27)$$

Using the 2×2 submatrices defined in Eq. (4) we write the dynamical matrix $\mathbf{M}_1^{(4)}$:

$$\mathbf{M}_1^{(4)} = \begin{bmatrix} -i\tilde{\gamma}_1 & \xi & 0 & 0 \\ \xi & -i\tilde{\gamma}_2 & \xi & 0 \\ 0 & \xi & -i\tilde{\gamma}_3 & \xi \\ 0 & 0 & \xi & -i\tilde{\gamma}_4 \end{bmatrix}. \quad (28)$$

The vectors $\hat{\mathbf{a}}$ of field operators and $\hat{\mathbf{L}}$ of the Langevin operator forces in Eq. (27) are given as $\hat{\mathbf{a}} = [\hat{a}_1, \hat{a}_2, \hat{a}_3, \hat{a}_4]^T \equiv [\hat{a}_1, \hat{a}_1^\dagger, \hat{a}_2, \hat{a}_2^\dagger, \hat{a}_3, \hat{a}_3^\dagger, \hat{a}_4, \hat{a}_4^\dagger]^T$ and $\hat{\mathbf{L}} = [\hat{L}_1, \hat{L}_1^\dagger, \hat{L}_2, \hat{L}_2^\dagger, \hat{L}_3, \hat{L}_3^\dagger, \hat{L}_4, \hat{L}_4^\dagger]^T$.

QEPs and QHPs have been found in the following two configurations:

1. Linear configuration with equal damping and/or amplification rates of neighbor modes

In this configuration schematically shown in Fig. 2(c) we assume equal damping and/or amplification rates in modes 1 and 2, and also modes 3 and 4:

$$\gamma_1 = \gamma_2 \equiv \gamma_{12}, \quad \gamma_3 = \gamma_4 \equiv \gamma_{34}. \quad (29)$$

In this case, diagonalization of the dynamical matrix $\mathbf{M}_{11}^{(4)}$ in Eq. (28) provides the eigenvalues

$$\begin{aligned} \lambda_{1,2}^{M_{11}^{(4)}} &= -i\gamma_+ \pm \alpha_-, \\ \lambda_{3,4}^{M_{11}^{(4)}} &= -i\gamma_+ \pm \alpha_+, \end{aligned} \quad (30)$$

and the corresponding eigenvectors

$$\begin{aligned} \mathbf{y}_{1,3}^{M_{11}^{(4)}} &= \left[-\frac{\delta_\pm^*}{2\xi^3}, \frac{\chi_\mp^{*2}}{\xi^2} - 1, \frac{\chi_\mp^*}{\xi}, 1 \right]^T, \\ \mathbf{y}_{2,4}^{M_{11}^{(4)}} &= \left[\frac{\delta_\pm}{2\xi^3}, \frac{\chi_\mp^2}{\xi^2} - 1, -\frac{\chi_\mp}{\xi}, 1 \right]^T. \end{aligned} \quad (31)$$

where $\delta_\pm = \xi^2(-2i\gamma_- + \chi_\mp) \pm 2\mu\chi_\mp$, $\chi_\pm = -i\gamma_+ + \alpha_\pm$, $\alpha_\pm^2 = \beta^2 \pm \mu$, $\beta^2 = 3\xi^2/2 - \gamma_-^2$, and $\mu^2 = 4\xi^2(5\xi^2/16 - \gamma_-^2)$ using $4\gamma_\pm = \gamma_{12} \pm \gamma_{34}$.

If $\mu = 0$ then $\alpha_+ = \alpha_-$ and $\chi_+ = \chi_-$. The eigenvalues in Eq. (30) are doubly degenerated: $\lambda_1^{M_{11}^{(4)}} = \lambda_3^{M_{11}^{(4)}}$ and $\lambda_2^{M_{11}^{(4)}} = \lambda_4^{M_{11}^{(4)}}$. The same holds also for their eigenvectors given in Eq. (31) and we have two QEPs with second-order ED. Similarly as in the case of three-mode

bosonic system, the inclusion of the structure of submatrices in the matrix $\mathbf{M}_{11}^{(4)}$ gives the second-order DD to these QEPs and we, thus, have two QHPs. They are localized at the ellipse

$$\frac{\kappa^2}{\epsilon^2} + \frac{16\gamma_-^2}{5\epsilon^2} = 1 \quad (32)$$

defined in the parameter space $(\kappa/\epsilon, \gamma_-/\epsilon)$. Real parts of the eigenvalues $\lambda_j^{M_{11}^{(4)}}$ for $j = 1, \dots, 4$ are drawn in this space in Fig. 2(c).

The eigenvalues and eigenvectors of the 8×8 matrix $\mathbf{M}_{11}^{(4)}$ obtained by merging those written in Eqs. (30) and (31) and Eqs. (7) and (8) for the matrix $\boldsymbol{\xi}$ (for details, see Appendix A) define the transformation into the new field operators $\hat{\mathbf{b}} = [\hat{b}_1, \hat{b}_2, \hat{b}_1^\dagger, \hat{b}_2^\dagger, \hat{b}_3, \hat{b}_4, \hat{b}_3^\dagger, \hat{b}_4^\dagger]^T$ in which the Heisenberg-Langevin equations have the diagonal form. This allows to reveal QEPs and QHPs in the dynamics of the first- and second-order FOMs. They are summarized in Tab. III.

2. Linear configuration with different damping and/or amplification rates for neighbor modes

We assume equal the damping and/or amplification rates in modes 1 and 3 and also in modes 2 and 4:

$$\gamma_1 = \gamma_3 \equiv \gamma_{13}, \quad \gamma_2 = \gamma_4 \equiv \gamma_{24}. \quad (33)$$

In this configuration, which is schematically depicted in Fig. 1(e), the eigenvalues of the 4×4 dynamical matrix $\mathbf{M}_{12}^{(4)}$ are obtained as follows:

$$\begin{aligned} \lambda_{1,2}^{M_{12}^{(4)}} &= -i\gamma_+ \pm \alpha_+, \\ \lambda_{3,4}^{M_{12}^{(4)}} &= -i\gamma_+ \pm \alpha_-. \end{aligned} \quad (34)$$

The corresponding eigenvectors are reached in the form:

$$\begin{aligned} \mathbf{y}_{1,3}^{M_{12}^{(4)}} &= \left[\frac{-\kappa_{\mp}}{\xi}, \kappa_{\pm}, \frac{\chi_{\pm}^*}{\xi}, 1 \right]^T, \\ \mathbf{y}_{2,4}^{M_{12}^{(4)}} &= \left[\frac{\kappa_{\mp}\chi_{\pm}}{\xi}, \kappa_{\pm}, -\frac{\chi_{\pm}}{\xi}, 1 \right]^T, \end{aligned} \quad (35)$$

where $\kappa_{\pm} = (\pm\sqrt{5}+1)/2$, $\chi_{\pm} = -i\gamma_+ + \alpha_{\pm}$, $\alpha_{\pm}^2 = \tilde{\beta} \pm \mu$, $\tilde{\beta} = 3\xi^2/2 - \gamma_-^2$, and $\mu = \sqrt{5}\xi^2/2$ using $4\gamma_{\pm} = \gamma_{13} \pm \gamma_{24}$.

Provided that $\alpha_+ = 0$ [$\alpha_- = 0$] the eigenvalues $\lambda_1^{M_{12}^{(4)}}$ and $\lambda_2^{M_{12}^{(4)}}$ [$\lambda_3^{M_{12}^{(4)}}$ and $\lambda_4^{M_{12}^{(4)}}$] in Eq. (34) and the eigenvectors $\mathbf{y}_1^{M_{12}^{(4)}}$ and $\mathbf{y}_2^{M_{12}^{(4)}}$ [$\mathbf{y}_3^{M_{12}^{(4)}}$ and $\mathbf{y}_4^{M_{12}^{(4)}}$] in Eq. (35) are equal to each other and we have a QEP with second-order ED. This means that, for the 8×8 dynamical matrix $\mathbf{M}_{12}^{(4)}$, we predict a QHP with second-order ED and DD

observed either for $\alpha_+ = 0$ or $\alpha_- = 0$. These conditions define two ellipses in the parameter space $(\kappa/\epsilon, \gamma_-/\epsilon)$,

$$\frac{\kappa^2}{\epsilon^2} + \frac{2\gamma_-^2}{(3 \pm \sqrt{5})\epsilon^2} = 1. \quad (36)$$

They are shown in Fig. 2(d) where the real parts of the eigenvalues $\lambda_j^{M_{12}^{(4)}}$ for $j = 1, \dots, 4$ are plotted.

The eigenvalues and eigenvectors of the 8×8 matrix $\mathbf{M}_{12}^{(4)}$, given in Appendix A, determine the transformation that leaves the Heisenberg-Langevin equations in their diagonal form. Thus, we define the new field operators $\hat{\mathbf{b}} = [\hat{b}_1, \hat{b}_2, \hat{b}_1^\dagger, \hat{b}_2^\dagger, \hat{b}_3, \hat{b}_4, \hat{b}_3^\dagger, \hat{b}_4^\dagger]^T$, whose evolution identifies the QEPs and QHPs in the first- and second-order FOM dynamics given in Tab. IV.

B. Circular configuration

In the circular configuration, the Hamiltonian $\hat{H}_{4,c}$ of four-mode system is expressed as

$$\begin{aligned} \hat{H}_{4,c} &= \left[\hbar\epsilon\hat{a}_1^\dagger\hat{a}_2 + \hbar\epsilon\hat{a}_2^\dagger\hat{a}_3 + \hbar\epsilon\hat{a}_3^\dagger\hat{a}_4 + \hbar\epsilon\hat{a}_4^\dagger\hat{a}_1 + \hbar\kappa\hat{a}_1\hat{a}_2 \right. \\ &\quad \left. + \hbar\kappa\hat{a}_2\hat{a}_3 + \hbar\kappa\hat{a}_3\hat{a}_4 + \hbar\kappa\hat{a}_4\hat{a}_1 \right] + \text{H.c.} \end{aligned} \quad (37)$$

Whereas the Heisenberg-Langevin equations keep the form of Eq. (27), the original dynamical matrix $\mathbf{M}_1^{(4)}$ of the linear configuration in Eq. (28) is modified into the form

$$\mathbf{M}_c^{(4)} = \begin{bmatrix} -i\tilde{\gamma}_1 & \xi & 0 & \xi \\ \xi & -i\tilde{\gamma}_2 & \xi & 0 \\ 0 & \xi & -i\tilde{\gamma}_3 & \xi \\ \xi & 0 & \xi & -i\tilde{\gamma}_4 \end{bmatrix}. \quad (38)$$

We derive the eigenvalues of the matrix $\mathbf{M}_c^{(4)}$ under the condition of the equal damping and/or amplification rates of the neighbor modes valid for the configuration plotted in Fig. 1(d); i.e.,

$$\gamma_1 = \gamma_2 \equiv \gamma_{12}, \quad \gamma_3 = \gamma_4 \equiv \gamma_{34}. \quad (39)$$

We obtain the following eigenvalues

$$\begin{aligned} \lambda_{1,2}^{M_c^{(4)}} &= -i\gamma_+ - \alpha_{\pm}, \\ \lambda_{3,4}^{M_c^{(4)}} &= -i\gamma_+ + \alpha_{\mp} \end{aligned} \quad (40)$$

that are accompanied by the following eigenvectors

$$\begin{aligned} \mathbf{y}_{1,2}^{M_c^{(4)}} &= \left[-\frac{\chi}{\xi}, \pm\frac{\chi}{\xi}, \mp 1, 1 \right]^T, \\ \mathbf{y}_{3,4}^{M_c^{(4)}} &= \left[\frac{\chi^*}{\xi}, \mp\frac{\chi^*}{\xi}, \mp 1, 1 \right]^T. \end{aligned} \quad (41)$$

The symbols introduced in Eqs. (40) and (41) are defined as $\chi = i\gamma_+ + \beta$, $\alpha_{\pm} = \beta \pm \xi$, $\beta^2 = \xi^2 - \gamma_-^2$, and $4\gamma_{\pm} = \gamma_{12} \pm \gamma_{34}$.

Λ_j^i	Λ_j^r	Moments		Moment deg.	Genuine and induced QHPs		Genuine QHPs	
					Partial QDP x QEP deg.	Partial QDP x QEP deg.	Partial QDP x QEP deg.	Partial QDP x QEP deg.
γ_+	α_{\pm}	$\langle b_1 \rangle, \langle b_3 \rangle$	$\langle \tilde{B}_1 \rangle$	1	2x2	4x2	2x2	4x2
		$\langle b_4 \rangle, \langle b_2 \rangle$	$\langle \tilde{B}_2 \rangle$	1				
	$-\alpha_{\pm}$	$\langle b_1^\dagger \rangle, \langle b_3^\dagger \rangle$	$\langle \tilde{B}_3 \rangle$	1	2x2		2x2	
		$\langle b_4^\dagger \rangle, \langle b_2^\dagger \rangle$	$\langle \tilde{B}_4 \rangle$	1				
$2\gamma_+$	$2\alpha_{\pm}$	$\langle b_1^2 \rangle, \langle b_3^2 \rangle$	$\langle \tilde{B}_1^2 \rangle$	1	1x4	16x4	1x3	4x3 +
	$\alpha_- + \alpha_+$	$\langle b_1 b_3 \rangle$		2				
	$2\alpha_{\mp}$	$\langle b_2^2 \rangle, \langle b_4^2 \rangle$	$\langle \tilde{B}_2^2 \rangle$	1	1x4		1x3	
	$\alpha_- + \alpha_+$	$\langle b_2 b_4 \rangle$		2				
	$-2\alpha_{\pm}$	$\langle b_1^{\dagger 2} \rangle, \langle b_3^{\dagger 2} \rangle$	$\langle \tilde{B}_3^2 \rangle$	1	1x4	1x3	6x4	
	$-\alpha_- - \alpha_+$	$\langle b_1^\dagger b_3^\dagger \rangle$		2				
	$-2\alpha_{\mp}$	$\langle b_2^{\dagger 2} \rangle, \langle b_4^{\dagger 2} \rangle$	$\langle \tilde{B}_4^2 \rangle$	1	1x4	1x3		
	$-\alpha_- - \alpha_+$	$\langle b_2^\dagger b_4^\dagger \rangle$		2				
	$-\alpha_{\pm} + \alpha_{\pm}$	$\langle b_1^\dagger b_1 \rangle, \langle b_3^\dagger b_3 \rangle$	$\langle \tilde{B}_3 \tilde{B}_1 \rangle$	2	2x4	1x4		
	$\pm \alpha_- \mp \alpha_+$	$\langle b_1^\dagger b_3 \rangle, \langle b_1 b_3^\dagger \rangle$		2				
	$-\alpha_{\mp} + \alpha_{\mp}$	$\langle b_2^\dagger b_2 \rangle, \langle b_4^\dagger b_4 \rangle$	$\langle \tilde{B}_4 \tilde{B}_2 \rangle$	2	2x4	1x4		
	$\mp \alpha_- \pm \alpha_+$	$\langle b_2^\dagger b_4 \rangle, \langle b_2 b_4^\dagger \rangle$		2				
	$\alpha_+ + \alpha_-$	$\langle b_1 b_2 \rangle, \langle b_3 b_4 \rangle$	$\langle \tilde{B}_1 \tilde{B}_2 \rangle$	2	2x4	1x4		
	$2\alpha_{\pm}$	$\langle b_1 b_4 \rangle, \langle b_3 b_2 \rangle$		2				
	$\alpha_{\mp} - \alpha_{\pm}$	$\langle b_1^\dagger b_2 \rangle, \langle b_3^\dagger b_4 \rangle$	$\langle \tilde{B}_3 \tilde{B}_2 \rangle$	2	2x4	1x4		
	$\alpha_{\pm} - \alpha_{\pm}$	$\langle b_1^\dagger b_4 \rangle, \langle b_3^\dagger b_2 \rangle$		2				
	$\alpha_{\pm} - \alpha_{\mp}$	$\langle b_2^\dagger b_1 \rangle, \langle b_4^\dagger b_3 \rangle$	$\langle \tilde{B}_4 \tilde{B}_1 \rangle$	2	2x4	1x4		
	$\alpha_{\pm} - \alpha_{\pm}$	$\langle b_4^\dagger b_1 \rangle, \langle b_2^\dagger b_3 \rangle$		2				
	$-\alpha_+ - \alpha_-$	$\langle b_1^\dagger b_2^\dagger \rangle, \langle b_3^\dagger b_4^\dagger \rangle$	$\langle \tilde{B}_3 \tilde{B}_4 \rangle$	2	2x4	1x4		
	$-2\alpha_{\pm}$	$\langle b_1^\dagger b_4^\dagger \rangle, \langle b_3^\dagger b_2^\dagger \rangle$		2				

TABLE III. Real and imaginary parts of the complex eigenfrequencies $\Lambda_j^r - i\Lambda_j^i$ of the matrix $M_{11}^{(4)}$, given in Eq. (28) with Eq. (29), for the linear four-mode bosonic system with equal damping and/or amplification rates for neighbor modes derived from the equations for the FOMs up to second order. We note that $\alpha_{\pm}(\zeta) = \alpha_{\mp}(-\zeta)$ is used here. For details, see the caption to Tab. I.

For $\beta = 0$, we have $\alpha_+ = -\alpha_-$ and $\chi^* = -\chi$. This leads to the relations $\lambda_1^{M_{c1}^{(4)}} = \lambda_3^{M_{c1}^{(4)}}$ and $\lambda_2^{M_{c1}^{(4)}} = \lambda_4^{M_{c1}^{(4)}}$. Also the corresponding eigenvectors coincide: $y_1^{M_{c1}^{(4)}} = y_3^{M_{c1}^{(4)}}$ and $y_2^{M_{c1}^{(4)}} = y_4^{M_{c1}^{(4)}}$. As a consequence, the two QEPs with second-order EDs occur. This means that the two QHPs with second-order EDs and DDs for the 8×8 matrix $M_{c1}^{(4)}$ are formed. These QHPs occur under the condition specified in Eq. (13) that identifies the QHPs in the analyzed two-mode bosonic system. The real values of the eigenvalues $\lambda_j^{M_{c1}^{(4)}}$ for $j = 1, \dots, 4$ are plotted in Fig. 2(e) together with the condition for the QHPs.

Using the eigenvalues and eigenvectors of the 4×4 matrix $M_{c1}^{(4)}$ and the 2×2 matrix ξ given in Eqs. (40), (41), (7), and (8), we arrive at the system dynamical matrix in its diagonal form (for details, see Appendix A). This brings us the new field operators $\hat{b} = [\hat{b}_1, \hat{b}_2, \hat{b}_3^\dagger, \hat{b}_4^\dagger, \hat{b}_3, \hat{b}_4, \hat{b}_1^\dagger, \hat{b}_2^\dagger]^T$ suitable for revealing QEPs and QHPs found in the dynamics of FOMs. As the structure of eigenvalues and eigenvectors is the same as that characterizing the four-mode linear system with equal damping and/or amplification rates of neighbor modes,

the appropriate QEPs and QHPs are given in Tab. III.

V. FIVE-MODE BOSONIC SYSTEMS

The largest bosonic systems in our investigations consist of five bosonic modes. Among them, QEPs and QHPs were identified in two configurations: linear and pyramid.

A. Linear configuration

A five-mode bosonic system in its linear configuration is depicted in Fig. 1(f). Its Hamiltonian $\hat{H}_{5,1}$ is given as follows:

$$\begin{aligned} \hat{H}_{5,1} = & \left[\hbar\epsilon\hat{a}_1^\dagger\hat{a}_2 + \hbar\epsilon\hat{a}_2^\dagger\hat{a}_3 + \hbar\epsilon\hat{a}_3^\dagger\hat{a}_4 + \hbar\epsilon\hat{a}_4^\dagger\hat{a}_5 + \hbar\kappa\hat{a}_1\hat{a}_2 \right. \\ & \left. + \hbar\kappa\hat{a}_2\hat{a}_3 + \hbar\kappa\hat{a}_3\hat{a}_4 + \hbar\kappa\hat{a}_4\hat{a}_5 \right] + \text{H.c.} \end{aligned} \quad (42)$$

Defining the vectors $\hat{a} = [\hat{a}_1, \hat{a}_2, \hat{a}_3, \hat{a}_4, \hat{a}_5]^T \equiv [\hat{a}_1, \hat{a}_1^\dagger, \hat{a}_2, \hat{a}_2^\dagger, \hat{a}_3, \hat{a}_3^\dagger, \hat{a}_4, \hat{a}_4^\dagger, \hat{a}_5, \hat{a}_5^\dagger]^T$ of field operators

Λ_j^i	Λ_j^r	Moments		Moment deg.	Genuine and induced QHPs		Genuine QHPs	
					Partial QDP x QEP deg.	Partial QDP x QEP deg.	Partial QDP x QEP deg.	Partial QDP x QEP deg.
γ_+	$\pm\alpha_+$	$\langle b_1 \rangle, \langle b_1^\dagger \rangle$	$\langle \tilde{B}_1 \rangle$	1	1x2	2x2	1x2	2x2
		$\langle b_2 \rangle, \langle b_2^\dagger \rangle$	$\langle \tilde{B}_2 \rangle$	1	1x2		1x2	
	α_-	$\langle b_3 \rangle$	$\langle \tilde{B}_3 \rangle$	1	2x1	2x1	2x1	2x1
		$\langle b_4 \rangle$	$\langle \tilde{B}_4 \rangle$	1				
	$-\alpha_-$	$\langle b_3^\dagger \rangle$	$\langle \tilde{B}_5 \rangle$	1	2x1	2x1	2x1	2x1
		$\langle b_4^\dagger \rangle$	$\langle \tilde{B}_6 \rangle$	1				
$2\gamma_+$	$\pm 2\alpha_+$	$\langle b_1^2 \rangle, \langle b_1^{\dagger 2} \rangle$	$\langle \tilde{B}_1^2 \rangle$	1	1x4	4x4	1x3	2x3 +
	$\alpha_+ - \alpha_+$	$\langle b_1^\dagger b_1 \rangle$		2				
	$\pm 2\alpha_+$	$\langle b_2^2 \rangle, \langle b_2^{\dagger 2} \rangle$	$\langle \tilde{B}_2^2 \rangle$	1	1x4		1x3	
	$\alpha_+ - \alpha_+$	$\langle b_2^\dagger b_2 \rangle$		2				
	$\pm\alpha_+$	$\langle b_1 b_2 \rangle, \langle b_1^\dagger b_2^\dagger \rangle$	$\langle \tilde{B}_1 \tilde{B}_2 \rangle$	2	2x4	16x2	1x4	1x4
	$\alpha_+ - \alpha_+$	$\langle b_1^\dagger b_2 \rangle, \langle b_1 b_2^\dagger \rangle$		2				
	$\alpha_- \pm \alpha_+$	$\langle b_1 b_3 \rangle, \langle b_1^\dagger b_3 \rangle$	$\langle \tilde{B}_1 \tilde{B}_3 \rangle$	2	2x2		2x2	
		$\langle b_1 b_4 \rangle, \langle b_1^\dagger b_4 \rangle$	$\langle \tilde{B}_1 \tilde{B}_4 \rangle$	2	2x2		2x2	
	$\alpha_- \pm \alpha_+$	$\langle b_2 b_3 \rangle, \langle b_2^\dagger b_3 \rangle$	$\langle \tilde{B}_2 \tilde{B}_3 \rangle$	2	2x2		2x2	
		$\langle b_2 b_4 \rangle, \langle b_2^\dagger b_4 \rangle$	$\langle \tilde{B}_2 \tilde{B}_4 \rangle$	2	2x2		2x2	
	$-\alpha_- \pm \alpha_+$	$\langle b_1 b_3^\dagger \rangle, \langle b_1^\dagger b_3^\dagger \rangle$	$\langle \tilde{B}_1 \tilde{B}_5 \rangle$	2	2x2		2x2	
		$\langle b_1 b_4^\dagger \rangle, \langle b_1^\dagger b_4^\dagger \rangle$	$\langle \tilde{B}_1 \tilde{B}_6 \rangle$	2	2x2		2x2	
	$-\alpha_- \pm \alpha_+$	$\langle b_2 b_3^\dagger \rangle, \langle b_2^\dagger b_3^\dagger \rangle$	$\langle \tilde{B}_2 \tilde{B}_5 \rangle$	2	2x2		2x2	
		$\langle b_2 b_4^\dagger \rangle, \langle b_2^\dagger b_4^\dagger \rangle$	$\langle \tilde{B}_2 \tilde{B}_6 \rangle$	2	2x2		2x2	
	$2\alpha_-$	$\langle b_3^2 \rangle, \langle b_4^2 \rangle$	$\langle \tilde{B}_3^2 \rangle, \langle \tilde{B}_4^2 \rangle$	1	4x1		3x1	
		$\langle b_3 b_4 \rangle$	$\langle \tilde{B}_3 \tilde{B}_4 \rangle$	2				
	$-2\alpha_-$	$\langle b_3^{\dagger 2} \rangle, \langle b_4^{\dagger 2} \rangle$	$\langle \tilde{B}_5^2 \rangle, \langle \tilde{B}_6^2 \rangle$	1	4x1		3x1	
		$\langle b_3 b_4^\dagger \rangle$	$\langle \tilde{B}_5 \tilde{B}_6 \rangle$	2				
	$\alpha_- - \alpha_-$	$\langle b_3^\dagger b_3 \rangle, \langle b_4^\dagger b_4 \rangle$	$\langle \tilde{B}_5 \tilde{B}_3 \rangle, \langle \tilde{B}_6 \tilde{B}_4 \rangle$	2	8x1		4x1	
		$\langle b_3^\dagger b_4 \rangle, \langle b_3 b_4^\dagger \rangle$	$\langle \tilde{B}_5 \tilde{B}_4 \rangle, \langle \tilde{B}_3 \tilde{B}_6 \rangle$	2				

TABLE IV. Real and imaginary parts of the complex eigenfrequencies $\Lambda_j^r - i\Lambda_j^i$ of the matrix $M_{12}^{(4)}$, given in Eq. (28) with Eq. (33) for the linear four-mode bosonic system with different damping and/or amplification rates of neighbor modes, as derived from the equations for the FOMs up to second order assuming $\alpha_+ = 0$. For details, see the caption to Tab. I.

and $\hat{L} = [\hat{L}_1, \hat{L}_1^\dagger, \hat{L}_2, \hat{L}_2^\dagger, \hat{L}_3, \hat{L}_3^\dagger, \hat{L}_4, \hat{L}_4^\dagger, \hat{L}_5, \hat{L}_5^\dagger]^T$ of the Langevin operator forces, we obtain the following Heisenberg-Langevin equations:

$$\frac{d\hat{a}}{dt} = -iM_1^{(5)}\hat{a} + \hat{L}. \quad (43)$$

The dynamical matrix $M_1^{(5)}$ introduced in Eq. (43) is written with the help of 2×2 submatrices introduced in Eq. (4) as

$$M_1^{(5)} = \begin{bmatrix} -i\tilde{\gamma}_1 & \xi & 0 & 0 & 0 \\ \xi & -i\tilde{\gamma}_2 & \xi & 0 & 0 \\ 0 & \xi & -i\tilde{\gamma}_3 & \xi & 0 \\ 0 & 0 & \xi & -i\tilde{\gamma}_4 & \xi \\ 0 & 0 & 0 & \xi & -i\tilde{\gamma}_5 \end{bmatrix}. \quad (44)$$

Motivated by \mathcal{PT} symmetry we assume:

$$\gamma_1 = \gamma_2 \equiv \gamma_{12}, \quad \gamma_4 = \gamma_5 \equiv \gamma_{45}. \quad (45)$$

Moreover, inspired by the condition in Eq. (22) derived for the three-mode linear system, we additionally assume:

$$2\gamma_3 = \gamma_{12} + \gamma_{45}. \quad (46)$$

Then, diagonalization of the matrix $M_1^{(5)}$ results in the following eigenvalues $\lambda_j^{M_1^{(5)}}$:

$$\begin{aligned} \lambda_1^{M_1^{(5)}} &= -i\gamma_+, \\ \lambda_{2,3}^{M_1^{(5)}} &= -i\gamma_+ \pm \alpha_-, \\ \lambda_{4,5}^{M_1^{(5)}} &= -i\gamma_+ \pm \alpha_+. \end{aligned} \quad (47)$$

The corresponding eigenvectors are derived as follows:

$$\begin{aligned} \mathbf{y}_1^{M_1^{(5)}} &= \left[1, \frac{i\gamma_-}{\xi}, -\frac{\gamma_-^2}{\xi^2} - 1, -\frac{i\gamma_-}{\xi}, 1 \right]^T, \\ \mathbf{y}_{2,4}^{M_1^{(5)}} &= \left[-1 \mp \frac{n_\mp}{4\xi^3}, -\frac{m_\mp}{\xi^3} \mp \frac{2\beta\chi_\mp}{\xi^2}, \frac{\chi_\mp^2}{\xi^2} - 1, \frac{\chi_\mp}{\xi}, 1 \right]^T, \\ \mathbf{y}_{3,5}^{M_1^{(5)}} &= \left[-1 \mp \frac{n_\mp^*}{4\xi^3}, \frac{m_\mp^*}{\xi^3} \pm \frac{2\beta\chi_\mp^*}{\xi^2}, \frac{\chi_\mp^{*2}}{\xi^2} - 1, -\frac{\chi_\mp^*}{\xi}, 1 \right]^T, \end{aligned} \quad (48)$$

where $n_\mp = (2\beta \mp \xi)[(2\beta \mp \xi)^2 - 4i\gamma_- \alpha_\mp]$, $m_\mp = i\gamma_- (\chi_\mp^2 + \xi^2)$, $\chi_\pm = -i\gamma_+ + \alpha_\pm$, $\alpha_\pm^2 = \beta^2 + 7\xi^2/4 \pm 2\beta\xi$, $\beta^2 = \xi^2/4 - \gamma_-^2$, and $4\gamma_\pm = \gamma_{12} \pm \gamma_{45}$.

If $\beta = 0$ then $\alpha_+ = \alpha_-$ and $\chi_+ = \chi_-$. Under these conditions, we have $\lambda_2^{M_1^{(5)}} = \lambda_4^{M_1^{(5)}}$ and $\mathbf{y}_2^{M_1^{(5)}} = \mathbf{y}_4^{M_1^{(5)}}$. We also have $\lambda_3^{M_1^{(5)}} = \lambda_5^{M_1^{(5)}}$ and $\mathbf{y}_3^{M_1^{(5)}} = \mathbf{y}_5^{M_1^{(5)}}$. Thus, we observe two QEPs with second-order EDs that give rise to two QHPs with second-order EDs and DDs when the 10×10 matrix $\mathbf{M}_1^{(5)}$ is analyzed. In the parameter space $(\kappa/\epsilon, \gamma_-/\epsilon)$, these QHPs are localized at the positions obeying the condition

$$\frac{\kappa^2}{\epsilon^2} + \frac{4\gamma_-^2}{\epsilon^2} = 1. \quad (49)$$

The real parts of the eigenvalues $\lambda_j^{M_1^{(5)}}$ forming QHPs ($j = 2, \dots, 5$) are plotted in Fig. 2(f).

The eigenvalues and eigenvectors of the 10×10 matrix $\mathbf{M}_1^{(5)}$ constructed from the formulas given in Eqs. (47) and (48) together with those in Eqs. (7) and (8) (for details, see Appendix A) allow us to describe the system dynamics via a diagonal dynamical matrix. The appropriate operators $\hat{\mathbf{b}} = [\hat{b}_1, \hat{b}_1^\dagger, \hat{b}_2, \hat{b}_3, \hat{b}_2^\dagger, \hat{b}_3^\dagger, \hat{b}_4, \hat{b}_5, \hat{b}_4^\dagger, \hat{b}_5^\dagger]^T$ then reveal QEPs and QHPs found in the dynamics of the first- and second-order FOMs (see Tab. V).

B. Pyramid configuration

Second-order QEPs and QHPs can also be identified in the pyramid configuration [the only considered non-planar configuration, see Fig. 1(g)] described by the following Hamiltonian $\hat{H}_{5,p}$:

$$\begin{aligned} \hat{H}_{5,p} = & \left[\hbar\epsilon\hat{a}_1^\dagger\hat{a}_2 + \hbar\epsilon\hat{a}_1^\dagger\hat{a}_4 + \hbar\epsilon\hat{a}_1^\dagger\hat{a}_5 + \hbar\epsilon\hat{a}_2^\dagger\hat{a}_3 + \hbar\epsilon\hat{a}_2^\dagger\hat{a}_5 \right. \\ & + \hbar\epsilon\hat{a}_3^\dagger\hat{a}_4 + \hbar\epsilon\hat{a}_3^\dagger\hat{a}_5 + \hbar\epsilon\hat{a}_4^\dagger\hat{a}_5 + \hbar\kappa\hat{a}_1\hat{a}_2 \\ & + \hbar\kappa\hat{a}_1\hat{a}_4 + \hbar\kappa\hat{a}_1\hat{a}_5 + \hbar\kappa\hat{a}_2\hat{a}_3 + \hbar\kappa\hat{a}_2\hat{a}_5 \\ & \left. + \hbar\kappa\hat{a}_3\hat{a}_4 + \hbar\kappa\hat{a}_3\hat{a}_5 + \hbar\kappa\hat{a}_4\hat{a}_5 \right] \text{H.c.} \end{aligned} \quad (50)$$

The Hamiltonian $\hat{H}_{5,p}$ given in Eq. (50) leads to the Heisenberg-Langevin equations (43) in which the dynamical matrix $\mathbf{M}_p^{(5)}$ attains the form using the 2×2 submatrices introduced in Eq. (4):

$$\mathbf{M}_p^{(5)} = \begin{bmatrix} -i\tilde{\gamma}_1 & \xi & 0 & \xi & \xi \\ \xi & -i\tilde{\gamma}_2 & \xi & 0 & \xi \\ 0 & \xi & -i\tilde{\gamma}_3 & \xi & \xi \\ \xi & 0 & \xi & -i\tilde{\gamma}_4 & \xi \\ \xi & \xi & \xi & \xi & -i\tilde{\gamma}_5 \end{bmatrix}. \quad (51)$$

Motivated by the \mathcal{PT} symmetry we assume:

$$\gamma_1 = \gamma_2 \equiv \gamma_{12}, \quad \gamma_3 = \gamma_4 \equiv \gamma_{34}. \quad (52)$$

Moreover, inspired by the condition (22) derived for the three-mode linear bosonic system, we additionally assume:

$$2\gamma_5 = \gamma_{12} + \gamma_{34}. \quad (53)$$

Under these conditions, diagonalization of the matrix $\mathbf{M}_p^{(5)}$ leaves us the following five eigenvalues $\lambda_j^{M_p^{(5)}}$:

$$\begin{aligned} \lambda_1^{M_p^{(5)}} &= -i\gamma_+, \\ \lambda_{2,3}^{M_p^{(5)}} &= -i\gamma_+ - \xi \pm \beta_1, \\ \lambda_{4,5}^{M_p^{(5)}} &= -i\gamma_+ + \xi \pm \beta_2. \end{aligned} \quad (54)$$

The corresponding eigenvectors are obtained as follows:

$$\begin{aligned} \mathbf{y}_1^{M_p^{(5)}} &= \left[\frac{-i\xi}{\gamma_-}, \frac{-i\xi}{\gamma_-}, \frac{i\xi}{\gamma_-}, \frac{i\xi}{\gamma_-}, 1 \right]^T, \\ \mathbf{y}_2^{M_p^{(5)}} &= \left[\frac{\chi_1}{\xi}, -\frac{\chi_1}{\xi}, -1, 1, 0 \right]^T, \\ \mathbf{y}_3^{M_p^{(5)}} &= \left[-\frac{\chi_1^*}{\xi}, \frac{\chi_1^*}{\xi}, -1, 1, 0 \right]^T, \\ \mathbf{y}_4^{M_p^{(5)}} &= [\sigma_+, \sigma_+, \sigma_+^8, \sigma_+^*, 1]^T, \\ \mathbf{y}_5^{M_p^{(5)}} &= [\sigma_-^*, \sigma_-^*, \sigma_-, \sigma_-, 1]^T, \end{aligned} \quad (55)$$

where $\sigma_\pm = (\xi \pm \chi_2)/(4\xi)$, $\beta_1^2 = \xi^2 - \gamma_-^2$, $\beta_2^2 = 5\xi^2 - \gamma_-^2$, $\chi_{1,2} = \beta_{1,2} - i\gamma_-$, and $4\gamma_\pm = \gamma_{12} \pm \gamma_{34}$.

Contrary to the eigenvalues of the models discussed above, the eigenvalues $\lambda_j^{M_p^{(5)}}$ for $j = 2, \dots, 5$ in Eq. (55) exhibit the linear dependence on ξ . This means that the DD inherited to all the above-discussed models is removed in this model. It remains only for the eigenvalue $\lambda_1^{M_p^{(5)}}$ that, however, has no ability to form EDs.

Provided that $\beta_1 = 0$, we have $\lambda_2^{M_p^{(5)}} = \lambda_3^{M_p^{(5)}}$ and $\mathbf{y}_2^{M_p^{(5)}} = \mathbf{y}_3^{M_p^{(5)}}$. Thus, we have the QEP with second-order ED. When the 10×10 matrix $\mathbf{M}_p^{(5)}$ is analyzed, there occur one second-order QEP for $\xi = \zeta$ and one second-order QEP for $\xi = -\zeta$. These QEPs occur in the parameter space $(\kappa/\epsilon, \gamma_-/\epsilon)$ under the condition written in Eq. (13).

Moreover, in parallel, if $\beta_2 = 0$, it holds that $\lambda_4^{M_p^{(5)}} = \lambda_5^{M_p^{(5)}}$ and $\mathbf{y}_4^{M_p^{(5)}} = \mathbf{y}_5^{M_p^{(5)}}$. Thus, similarly as above, we observe the QEP with second-order ED for the 5×5 matrix $\mathbf{M}_p^{(5)}$. There occur one second-order QEP for $\xi = \zeta$ and one second-order QEP for $\xi = -\zeta$ for the 10×10 matrix $\mathbf{M}_p^{(5)}$. These QEPs are localized in the parameter space $(\kappa/\epsilon, \gamma_-/\epsilon)$ at the points fulfilling the condition:

$$\frac{\kappa^2}{\epsilon^2} + \frac{\gamma_-^2}{5\epsilon^2} = 1. \quad (56)$$

The real parts of the eigenvalues $\lambda_j^{M_p^{(5)}}$ forming QEPs ($j = 2, \dots, 5$) are drawn in Fig. 2(g,h).

We note that for $\xi = 0$ (i.e., $\gamma_- = 0$, $\kappa = \epsilon$) we have a specific QHP with ten-fold frequency degeneracy that belongs to four doubly-degenerate eigenvectors and another two eigenvectors.

Λ_j^i	Λ_j^r	Moments		Moment deg.	Genuine and induced QHPs		Genuine QHPs			
					Partial QDP x QEP deg.	Partial QDP x QEP deg.	Partial QDP x QEP deg.	Partial QDP x QEP deg.		
γ_+	α_\mp	$\langle b_2 \rangle, \langle b_4 \rangle$	$\langle \tilde{B}_1 \rangle$	1	2x2	4x2	2x2	4x2		
		$\langle b_3 \rangle, \langle b_5 \rangle$	$\langle \tilde{B}_2 \rangle$	1						
	$-\alpha_\mp$	$\langle b_2^\dagger \rangle, \langle b_4^\dagger \rangle$	$\langle \tilde{B}_3 \rangle$	1	2x2		2x2			
		$\langle b_3^\dagger \rangle, \langle b_5^\dagger \rangle$	$\langle \tilde{B}_4 \rangle$	1						
	0	$\langle b_1 \rangle$	$\langle \tilde{B}_5 \rangle$	1	2x1	2x1	2x1	2x1		
		$\langle b_1^\dagger \rangle$	$\langle \tilde{B}_6 \rangle$	1						
$2\gamma_+$	$2\alpha_\mp$	$\langle b_2^2 \rangle, \langle b_4^2 \rangle$	$\langle \tilde{B}_1^2 \rangle$	1	1x4	16x4	1x3	4x3 +		
	$\alpha_- + \alpha_+$	$\langle b_2 b_4 \rangle$		2						
	$2\alpha_\mp$	$\langle b_3^2 \rangle, \langle b_5^2 \rangle$	$\langle \tilde{B}_2^2 \rangle$	1	1x4		1x3			
	$\alpha_- + \alpha_+$	$\langle b_3 b_5 \rangle$		2						
	$-2\alpha_\mp$	$\langle b_2^{\dagger 2} \rangle, \langle b_4^{\dagger 2} \rangle$	$\langle \tilde{B}_3^2 \rangle$	1	1x4		1x3			
	$-\alpha_- - \alpha_+$	$\langle b_2^\dagger b_4^\dagger \rangle$		2						
	$-2\alpha_\mp$	$\langle b_3^{\dagger 2} \rangle, \langle b_5^{\dagger 2} \rangle$	$\langle \tilde{B}_4^2 \rangle$	1	1x4		1x3			
	$-\alpha_- - \alpha_+$	$\langle b_3^\dagger b_5^\dagger \rangle$		2						
	$2\alpha_\mp$	$\langle b_2 b_3 \rangle, \langle b_4 b_5 \rangle$	$\langle \tilde{B}_1 \tilde{B}_2 \rangle$	2	2x4		1x4			
	$\alpha_+ + \alpha_-$	$\langle b_2 b_5 \rangle, \langle b_4 b_3 \rangle$		2						
	$-\alpha_\mp + \alpha_\mp$	$\langle b_2^\dagger b_2 \rangle, \langle b_4^\dagger b_4 \rangle$	$\langle \tilde{B}_3 \tilde{B}_1 \rangle$	2	2x4		1x4			
	$-\alpha_\mp + \alpha_\pm$	$\langle b_2^\dagger b_4 \rangle, \langle b_2 b_4^\dagger \rangle$		2						
	$\alpha_\mp - \alpha_\mp$	$\langle b_3^\dagger b_2 \rangle, \langle b_5^\dagger b_4 \rangle$	$\langle \tilde{B}_4 \tilde{B}_1 \rangle$	2	2x4		1x4			
	$\alpha_\pm - \alpha_\mp$	$\langle b_5^\dagger b_2 \rangle, \langle b_3^\dagger b_4 \rangle$		2						
	$\alpha_\mp - \alpha_\mp$	$\langle b_2^\dagger b_3 \rangle, \langle b_4^\dagger b_5 \rangle$	$\langle \tilde{B}_3 \tilde{B}_2 \rangle$	2	2x4		1x4			
	$\alpha_\pm - \alpha_\mp$	$\langle b_2^\dagger b_5 \rangle, \langle b_4^\dagger b_3 \rangle$		2						
	$-\alpha_\mp + \alpha_\mp$	$\langle b_3^\dagger b_3 \rangle, \langle b_5^\dagger b_5 \rangle$	$\langle \tilde{B}_4 \tilde{B}_2 \rangle$	2	2x4		1x4			
	$-\alpha_\mp + \alpha_\pm$	$\langle b_3^\dagger b_5 \rangle, \langle b_5^\dagger b_3 \rangle$		2						
	$-2\alpha_\mp$	$\langle b_2^\dagger b_3^\dagger \rangle, \langle b_4^\dagger b_5^\dagger \rangle$	$\langle \tilde{B}_3 \tilde{B}_4 \rangle$	2	2x4		1x4			
	$-\alpha_+ - \alpha_-$	$\langle b_2^\dagger b_5^\dagger \rangle, \langle b_4^\dagger b_3^\dagger \rangle$		2						
	α_\mp	$\langle b_2 b_1 \rangle, \langle b_4 b_1 \rangle$	$\langle \tilde{B}_1 \tilde{B}_5 \rangle$	2	8x2	16x2	4x2	8x2		
		$\langle b_2 b_1^\dagger \rangle, \langle b_4 b_1^\dagger \rangle$	$\langle \tilde{B}_1 \tilde{B}_6 \rangle$	2						
		$\langle b_3 b_1 \rangle, \langle b_5 b_1 \rangle$	$\langle \tilde{B}_2 \tilde{B}_5 \rangle$	2						
		$\langle b_3 b_1^\dagger \rangle, \langle b_5 b_1^\dagger \rangle$	$\langle \tilde{B}_2 \tilde{B}_6 \rangle$	2						
	$-\alpha_\mp$	$\langle b_2^\dagger b_4 \rangle, \langle b_4^\dagger b_1 \rangle$	$\langle \tilde{B}_3 \tilde{B}_5 \rangle$	2	8x2				4x2	
		$\langle b_2^\dagger b_1^\dagger \rangle, \langle b_4^\dagger b_1^\dagger \rangle$	$\langle \tilde{B}_3 \tilde{B}_6 \rangle$	2						
		$\langle b_3^\dagger b_1 \rangle, \langle b_5^\dagger b_1 \rangle$	$\langle \tilde{B}_4 \tilde{B}_5 \rangle$	2						
		$\langle b_3^\dagger b_1^\dagger \rangle, \langle b_5^\dagger b_1^\dagger \rangle$	$\langle \tilde{B}_4 \tilde{B}_6 \rangle$	2						
0	$\langle b_1^2 \rangle, \langle b_1^{\dagger 2} \rangle$	$\langle \tilde{B}_5^2 \rangle, \langle \tilde{B}_6^2 \rangle$	1	4x1	4x1	3x1	3x1			
	$\langle b_1^\dagger b_1 \rangle$	$\langle \tilde{B}_6 \tilde{B}_5 \rangle$	2							

TABLE V. Real and imaginary parts of the complex eigenfrequencies $\Lambda_j^r - i\Lambda_j^i$ of the matrix $\mathbf{M}_1^{(5)}$, given in Eq. (44), for the five-mode linear bosonic system derived from the equations for the FOMs up to second order. For details, see the caption to Tab. I.

The eigenvalues and eigenvectors of the 10×10 matrix $\mathbf{M}_P^{(5)}$ formed from the expressions given in Eqs. (54) and (55) and also in Eqs. (7) and (8) (for details, see Appendix A) allow us to analyze the system dynamics via a diagonal dynamical matrix. The appropriate operators $\hat{\mathbf{b}} = [\hat{b}_1, \hat{b}_1^\dagger, \hat{b}_2, \hat{b}_3, \hat{b}_3^\dagger, \hat{b}_2^\dagger, \hat{b}_4, \hat{b}_5, \hat{b}_5^\dagger, \hat{b}_4^\dagger]^T$ then allow to identify the QEPs and QHPs observed in the dynamics of the first- and second-order FOMs, as summarized in Tab. VI).

VI. CONCLUSIONS

We have analyzed the dynamics of simple bosonic systems described by quadratic non-Hermitian Hamiltonians from the point of view of the occurrence of quantum exceptional, diabolical, and hybrid points. Non-Hermiticity of the considered systems, composed of from two to five coupled modes, originated in their damping and/or amplification, that are accompanied by the corresponding Langevin fluctuating forces to assure the physically consistent behavior. We have identified specific configurations defined by two-mode couplings and conditions for the damping and amplification rates of the modes at

Λ_j^i	Λ_j^r	Moments		Moment deg.	Genuine and induced QHPs		Genuine QHPs	
					Partial QDP x QEP deg.	Partial QDP x QEP deg.	Partial QDP x QEP deg.	Partial QDP x QEP deg.
γ_+	$-\zeta \mp \beta_2$	$\langle b_4 \rangle, \langle b_5^\dagger \rangle$	$\langle \tilde{B}_1 \rangle$	1	1x2	1x2	1x2	1x2
	$\zeta \pm \beta_2$	$\langle b_4^\dagger \rangle, \langle b_5 \rangle$	$\langle \tilde{B}_2 \rangle$	1	1x2	1x2	1x2	1x2
	$\zeta - \beta_1$	$\langle b_2 \rangle$	$\langle \tilde{B}_3 \rangle$	1	1x1	1x1	1x1	1x1
	$-\zeta + \beta_1$	$\langle b_2^\dagger \rangle$	$\langle \tilde{B}_4 \rangle$	1	1x1	1x1	1x1	1x1
	$-\zeta - \beta_1$	$\langle b_3 \rangle$	$\langle \tilde{B}_5 \rangle$	1	1x1	1x1	1x1	1x1
	$\zeta + \beta_1$	$\langle b_3^\dagger \rangle$	$\langle \tilde{B}_6 \rangle$	1	1x1	1x1	1x1	1x1
	0	$\langle b_1 \rangle$	$\langle \tilde{B}_7 \rangle$	1	2x1	2x1	2x1	2x1
		$\langle b_1^\dagger \rangle$	$\langle \tilde{B}_8 \rangle$	1				
$2\gamma_+$	$-2\zeta \mp 2\beta_2$	$\langle b_4^2 \rangle, \langle b_5^{\dagger 2} \rangle$	$\langle \tilde{B}_1^2 \rangle$	1	1x4	1x4	1x3	1x3
	-2ζ	$\langle b_5^\dagger b_4 \rangle$		2				
	$2\zeta \pm 2\beta_2$	$\langle b_4^{\dagger 2} \rangle, \langle b_5^2 \rangle$	$\langle \tilde{B}_2^2 \rangle$	1	1x4	1x4	1x3	1x3
	2ζ	$\langle b_4^\dagger b_5 \rangle$		2				
	$2\zeta - 2\beta_1$	$\langle b_2^2 \rangle$	$\langle \tilde{B}_3^2 \rangle$	1	1x1	1x1	1x1	1x1
	$-2\zeta + 2\beta_1$	$\langle b_2^{\dagger 2} \rangle$	$\langle \tilde{B}_4^2 \rangle$	1	1x1	1x1	1x1	1x1
	$-2\zeta - 2\beta_1$	$\langle b_3^2 \rangle$	$\langle \tilde{B}_5^2 \rangle$	1	1x1	1x1	1x1	1x1
	$2\zeta + 2\beta_1$	$\langle b_3^{\dagger 2} \rangle$	$\langle \tilde{B}_6^2 \rangle$	1	1x1	1x1	1x1	1x1
	0	$\langle b_1^2 \rangle, \langle b_1^{\dagger 2} \rangle$	$\langle \tilde{B}_7^2 \rangle, \langle \tilde{B}_8^2 \rangle$	1	4x1	4x1	3x1	3x1
		$\langle b_1^\dagger b_1 \rangle$	$\langle \tilde{B}_8 \tilde{B}_7 \rangle$	2				
	$\pm 2\beta_2$	$\langle b_4^\dagger b_5^\dagger \rangle, \langle b_4 b_5 \rangle$	$\langle \tilde{B}_2 \tilde{B}_1 \rangle$	2	2x4	2x4	1x4	1x4
	$\beta_2 - \beta_2$	$\langle b_4^\dagger b_4 \rangle, \langle b_5 b_5^\dagger \rangle$		2				
	$-\beta_1 \mp \beta_2$	$\langle b_4 b_2 \rangle, \langle b_5^\dagger b_2 \rangle$	$\langle \tilde{B}_1 \tilde{B}_3 \rangle$	2	4x1	4x1	2x1	2x1
	$2\zeta - \beta_1 \pm \beta_2$	$\langle b_4^\dagger b_2 \rangle, \langle b_5 b_2 \rangle$	$\langle \tilde{B}_2 \tilde{B}_3 \rangle$	2	4x1	4x1	2x1	2x1
	$-2\zeta + \beta_1 \mp \beta_2$	$\langle b_2^\dagger b_4 \rangle, \langle b_2^\dagger b_5^\dagger \rangle$	$\langle \tilde{B}_4 \tilde{B}_1 \rangle$	2	4x1	4x1	2x1	2x1
	$\beta_1 \pm \beta_2$	$\langle b_2^\dagger b_4^\dagger \rangle, \langle b_2^\dagger b_5 \rangle$	$\langle \tilde{B}_4 \tilde{B}_2 \rangle$	2	4x1	4x1	2x1	2x1
	$-2\zeta - \beta_1 \mp \beta_2$	$\langle b_4 b_3 \rangle, \langle b_5^\dagger b_3 \rangle$	$\langle \tilde{B}_1 \tilde{B}_5 \rangle$	2	4x1	4x1	2x1	2x1
	$-\beta_1 \pm \beta_2$	$\langle b_4^\dagger b_3 \rangle, \langle b_5 b_3 \rangle$	$\langle \tilde{B}_2 \tilde{B}_5 \rangle$	2	4x1	4x1	2x1	2x1
	$\beta_1 \mp \beta_2$	$\langle b_3^\dagger b_4 \rangle, \langle b_3^\dagger b_5^\dagger \rangle$	$\langle \tilde{B}_6 \tilde{B}_1 \rangle$	2	4x1	4x1	2x1	2x1
	$2\zeta + \beta_1 \pm \beta_2$	$\langle b_3^\dagger b_4^\dagger \rangle, \langle b_3^\dagger b_5 \rangle$	$\langle \tilde{B}_6 \tilde{B}_2 \rangle$	2	4x1	4x1	2x1	2x1
	$-\zeta \mp \beta_2$	$\langle b_4 b_1 \rangle, \langle b_5^\dagger b_1 \rangle$	$\langle \tilde{B}_7 \tilde{B}_1 \rangle$	2	4x2	4x2	2x2	2x2
		$\langle b_4 b_1^\dagger \rangle, \langle b_5^\dagger b_1^\dagger \rangle$	$\langle \tilde{B}_8 \tilde{B}_1 \rangle$	2				
	$\zeta \pm \beta_2$	$\langle b_4^\dagger b_1 \rangle, \langle b_5 b_1 \rangle$	$\langle \tilde{B}_7 \tilde{B}_2 \rangle$	2	4x2	4x2	2x2	2x2
		$\langle b_4^\dagger b_1^\dagger \rangle, \langle b_5 b_1^\dagger \rangle$	$\langle \tilde{B}_8 \tilde{B}_2 \rangle$	2				
	$\beta_1 - \beta_1$	$\langle b_2^\dagger b_2 \rangle$	$\langle \tilde{B}_4 \tilde{B}_3 \rangle$	2	2x1	2x1	1x1	1x1
	$-2\beta_1$	$\langle b_3 b_2 \rangle$	$\langle \tilde{B}_5 \tilde{B}_3 \rangle$	2	2x1	2x1	1x1	1x1
	2ζ	$\langle b_3^\dagger b_2 \rangle$	$\langle \tilde{B}_6 \tilde{B}_3 \rangle$	2	2x1	2x1	1x1	1x1
	$\zeta - \beta_1$	$\langle b_1 b_2 \rangle$	$\langle \tilde{B}_7 \tilde{B}_3 \rangle$	2	4x1	4x1	2x1	2x1
		$\langle b_1^\dagger b_2 \rangle$	$\langle \tilde{B}_8 \tilde{B}_3 \rangle$	2				
	-2ζ	$\langle b_2^\dagger b_3 \rangle$	$\langle \tilde{B}_4 \tilde{B}_5 \rangle$	2	2x1	2x1	1x1	1x1
	$2\beta_1$	$\langle b_2^\dagger b_3^\dagger \rangle$	$\langle \tilde{B}_4 \tilde{B}_6 \rangle$	2	2x1	2x1	1x1	1x1
	$-\zeta - \beta_1$	$\langle b_2^\dagger b_1 \rangle$	$\langle \tilde{B}_4 \tilde{B}_7 \rangle$	2	4x1	4x1	2x1	2x1
		$\langle b_2^\dagger b_1^\dagger \rangle$	$\langle \tilde{B}_4 \tilde{B}_8 \rangle$	2				
	$\beta_1 - \beta_1$	$\langle b_3^\dagger b_3 \rangle$	$\langle \tilde{B}_6 \tilde{B}_5 \rangle$	2	2x1	2x1	1x1	1x1
	$-\zeta - \beta_1$	$\langle b_1 b_3 \rangle$	$\langle \tilde{B}_7 \tilde{B}_5 \rangle$	2	4x1	4x1	2x1	2x1
		$\langle b_1^\dagger b_3 \rangle$	$\langle \tilde{B}_8 \tilde{B}_5 \rangle$	2				
	$\zeta + \beta_1$	$\langle b_3^\dagger b_1 \rangle$	$\langle \tilde{B}_6 \tilde{B}_7 \rangle$	2	4x1	4x1	2x1	2x1
		$\langle b_3^\dagger b_1^\dagger \rangle$	$\langle \tilde{B}_6 \tilde{B}_8 \rangle$	2				

TABLE VI. Real and imaginary parts of the complex eigenfrequencies $\Lambda_j^i - i\Lambda_j^i$ of the matrix $M_P^{(5)}$, given in Eq. (51), for the five-mode pyramid bosonic system derived from the equations for the FOMs up to second order assuming $\beta_2 = 0$. For details, see the caption to Tab. I. If $\beta_1 = 0$ instead of $\beta_2 = 0$, simple relabelling of b_j, b_j^\dagger operators provides the corresponding table.

which the inherited quantum exceptional and diabolical points occur. Surprisingly, in these physically consistent models, we have found only second- and third-order inherited quantum exceptional points including their doubling due to second-order diabolical degeneracies. We have shown in general that the analyzed bosonic systems naturally exhibit these second-order diabolical degeneracies. The exceptional and diabolical degeneracies of inherited quantum hybrid points have then been used to construct higher-order degeneracies observed in the dynamics of second-order field-operator moments. The corresponding quantum exceptional and hybrid points are summarized in tables that demonstrate a rich structure of the evolution of the general-order field-operator moments.

The investigations have revealed the need for further looking for the bosonic systems with higher-order inherited quantum exceptional and hybrid points by weakening the requirements to the considered systems. In Ref. [50] we extend our investigations to bosonic systems with partial \mathcal{PT} -symmetry like dynamics (nonconventional \mathcal{PT} -symmetry) as well as non-Hermitian bosonic systems with unidirectional coupling.

We may conclude in general that the performed analysis opens the door for further detailed investigations of the role of exceptional and diabolical degeneracies responsible for inducing unusual physical effects observed in physically well-behaved systems at exceptional, diabolical, and hybrid points.

VII. ACKNOWLEDGEMENTS

The authors thank Ievgen I. Arkhipov for useful discussions. J.P. and K.T. acknowledge support by the project OP JAC CZ.02.01.01/00/22_008/0004596 of the Ministry of Education, Youth, and Sports of the Czech Republic. A.K.-K., G.Ch., and A.M. were supported by the Polish National Science Centre (NCN) under the Maestro Grant No. DEC-2019/34/A/ST2/00081.

Appendix A: Eigenvalues and eigenvectors of three-, four- and five-mode bosonic systems

In this Appendix, we present the eigenvalues and eigenvectors of the dynamical matrices of the Heisenberg-Langevin equations for the three-, four-, and five-mode bosonic systems in configurations depicted in Fig. 1.

1. General n -mode bosonic systems

The eigenvalues of the $2n \times 2n$ dynamical matrix $\mathbf{M}^{(n)}$ belonging to a system with n modes ($n = 2, 3, \dots$) are constructed from the eigenvalues $\lambda_j^{M^{(n)}}$, $j = 1, \dots, n$, derived for the form of the dynamical matrix containing

2×2 submatrices and the eigenvalues λ_j^ξ , $j = 1, 2$, of the matrix ξ given in Eq. (7) as follows:

$$\begin{aligned}\Lambda_{2j-1}^{M^{(n)}} &= \lambda_j^{M^{(n)}} (\xi = \lambda_1^\xi), \\ \Lambda_{2j}^{M^{(n)}} &= \lambda_j^{M^{(n)}} (\xi = \lambda_2^\xi), \quad j = 1, 2, \dots, n.\end{aligned}\quad (\text{A1})$$

Similarly, using the corresponding eigenvectors $\mathbf{y}_j^{M^{(n)}}$ of the $n \times n$ matrix $\mathbf{M}^{(n)}$ formed by submatrices and the eigenvectors \mathbf{y}_j^ξ , $j = 1, 2$, of the matrix ξ in Eq. (8), we arrive at the following eigenvectors of the $2n \times 2n$ matrix $\mathbf{M}^{(n)}$ associated with the eigenvalues given in Eq. (A1):

$$\begin{aligned}\mathbf{Y}_{2j-1}^{M^{(n)}} &= \begin{bmatrix} y_{j,1}^{M^{(n)}} (\xi = \lambda_1^\xi) \mathbf{y}_1^\xi \\ y_{j,2}^{M^{(n)}} (\xi = \lambda_1^\xi) \mathbf{y}_1^\xi \\ \vdots \\ y_{j,n}^{M^{(n)}} (\xi = \lambda_1^\xi) \mathbf{y}_1^\xi \end{bmatrix}, \\ \mathbf{Y}_{2j}^{M^{(n)}} &= \begin{bmatrix} y_{j,1}^{M^{(n)}} (\xi = \lambda_2^\xi) \mathbf{y}_2^\xi \\ y_{j,2}^{M^{(n)}} (\xi = \lambda_2^\xi) \mathbf{y}_2^\xi \\ \vdots \\ y_{j,n}^{M^{(n)}} (\xi = \lambda_2^\xi) \mathbf{y}_2^\xi \end{bmatrix}, \quad j = 1, \dots, n.\end{aligned}\quad (\text{A2})$$

2. Three-mode bosonic system

In the three-mode system ($n = 3$) assuming $\beta = \sqrt{2\zeta^2 - \gamma_-^2} = 0$, we find a QHP with third-order ED and second-order DD. All the eigenvalues in Eq. (A1) are the same in this case and the eigenvectors in Eq. (A2) obey the relations $\mathbf{Y}_1^{M^{(3)}} = \mathbf{Y}_3^{M^{(3)}} = \mathbf{Y}_5^{M^{(3)}}$ and $\mathbf{Y}_2^{M^{(3)}} = \mathbf{Y}_4^{M^{(3)}} = \mathbf{Y}_6^{M^{(3)}}$.

3. Four-mode bosonic systems

In the four-mode system ($n = 4$) in the linear configuration with equal damping and/or amplification rates of neighbor modes and assuming $\mu = 2\sqrt{\zeta^2(5\zeta^2/16 - \gamma_-^2)} = 0$, we observe two QHPs with second-order ED and second-order DD. The eigenvalues $\Lambda_{11}^{M^{(4)}}$ and also the eigenvalues $\Lambda_{3,4,7,8}^{M^{(4)}}$ in Eq. (A1) coincide. The eigenvectors in Eq. (A2) obey the relations $\mathbf{Y}_j^{M^{(4)}} = \mathbf{Y}_{j+4}^{M^{(4)}}$ for $j = 1, \dots, 4$.

In the four-mode system ($n = 4$) in the linear configuration with different damping and/or amplification rates in neighbor modes and assuming $\alpha_+ = 0$ [$\alpha_- = 0$], $\alpha_\pm = \sqrt{(3 \pm \sqrt{5})\zeta^2/2 - \gamma_-^2} = 0$, we find a single QHP with second-order ED and DD. The eigenvalues $\Lambda_{1,2,3,4}^{M^{(4)}}$ [$\Lambda_{5,6,7,8}^{M^{(4)}}$] in Eq. (A1) are equal. The eigenvectors in Eq. (A2) fulfil: $\mathbf{Y}_1^{M^{(4)}} = \mathbf{Y}_3^{M^{(4)}}$ and $\mathbf{Y}_2^{M^{(4)}} = \mathbf{Y}_4^{M^{(4)}}$ [$\mathbf{Y}_5^{M^{(4)}} = \mathbf{Y}_7^{M^{(4)}}$ and $\mathbf{Y}_6^{M^{(4)}} = \mathbf{Y}_8^{M^{(4)}}$].

In the four-mode system ($n = 4$) in the circular configuration with equal damping and/or amplification rates of neighbor modes and assuming $\beta = \sqrt{\zeta^2 - \gamma_-^2} = 0$, we have two QHPs with second-order EDs and second-order DDs. The eigenvalues and eigenvectors in this case behave analogous to those given above for the four-mode system in the linear configuration with equal damping and/or amplification rates of neighbor modes.

4. Five-mode bosonic systems

In the five-mode system ($n = 5$) in the linear configuration and assuming $\beta = \sqrt{\zeta^2/4 - \gamma_-^2} = 0$, we have two QHPs with second-order EDs and second-order DDs. The eigenvalues $\Lambda_{3,4,7,8}^{M_1^{(5)}}$ and also the eigenvalues $\Lambda_{5,6,9,10}^{M_1^{(5)}}$ in Eq. (A1) are the same. The eigenvectors in Eq. (A2) fulfill the relations: $\mathbf{Y}_3^{M_1^{(5)}} = \mathbf{Y}_7^{M_1^{(5)}}$, $\mathbf{Y}_4^{M_1^{(5)}} = \mathbf{Y}_8^{M_1^{(5)}}$,

$$\mathbf{Y}_5^{M_1^{(5)}} = \mathbf{Y}_9^{M_1^{(5)}}, \text{ and } \mathbf{Y}_6^{M_1^{(5)}} = \mathbf{Y}_{10}^{M_1^{(5)}}.$$

In the five-mode system ($n = 5$) in the pyramid configuration and assuming $\beta_1 = \sqrt{\zeta^2 - \gamma_-^2} = 0$, we have two QEPs with second-order ED. The eigenvalues $\Lambda_3^{M_p^{(5)}}$ and $\Lambda_5^{M_p^{(5)}}$ together with their accompanying eigenvectors $\mathbf{Y}_3^{M_p^{(5)}} = \mathbf{Y}_5^{M_p^{(5)}}$ coincide. The same is true for eigenvalues $\Lambda_4^{M_p^{(5)}}$ and $\Lambda_6^{M_p^{(5)}}$ and eigenvectors $\mathbf{Y}_4^{M_p^{(5)}}$ and $\mathbf{Y}_6^{M_p^{(5)}}$. Provided that $\beta_2 = \sqrt{5\zeta^2 - \gamma_-^2} = 0$, we reveal two QEPs with second-order ED. The eigenvalues $\Lambda_7^{M_p^{(5)}}$ and $\Lambda_9^{M_p^{(5)}}$ together with their accompanying eigenvectors $\mathbf{Y}_7^{M_p^{(5)}}$ and $\mathbf{Y}_9^{M_p^{(5)}}$ are the same. Similarly, the eigenvalues $\Lambda_8^{M_p^{(5)}}$ and $\Lambda_{10}^{M_p^{(5)}}$ and eigenvectors $\mathbf{Y}_8^{M_p^{(5)}}$ and $\mathbf{Y}_{10}^{M_p^{(5)}}$ equal.

-
- [1] C. M. Bender and S. Boettcher, Real spectra in non-Hermitian Hamiltonians having \mathcal{PT} symmetry, Phys. Rev. Lett. **80**, 5243 (1998).
 - [2] C. M. Bender, D. C. Brody, and H. F. Jones, Must a Hamiltonian be Hermitian?, Am. J. Phys. **71**, 1095 (2003).
 - [3] C. M. Bender, Making sense of non-Hermitian Hamiltonians, Contemp. Phys. **70**, 947 (2007).
 - [4] R. El-Ganainy, K. G. Makris, M. Khajavikhan, Z. H. Musslimani, S. Rotter, and D. N. Christodoulides, Non-Hermitian physics and \mathcal{PT} symmetry, Nat. Phys. **14**, 11 (2018).
 - [5] Y. Ashida, Z. Gong, and M. Ueda, Non-Hermitian physics, Adv. Phys. **69**, 249 (2020).
 - [6] A. Mostafazadeh, Pseudo-Hermiticity and generalized \mathcal{PT} and \mathcal{CPT} -symmetries, J. Math. Phys. (Melville, NY) **44**, 974 (2003).
 - [7] A. Mostafazadeh, Time dependent Hilbert spaces, geometric phases, and general covariance in quantum mechanics, Phys. Lett. A **320**, 375 (2004).
 - [8] A. Mostafazadeh, Pseudo-Hermitian representation of quantum mechanics, Int. J. Geom. Meth. Mod. Phys. **7**, 1191 (2010).
 - [9] M. Znojil, Time-dependent version of crypto-Hermitian quantum theory, Phys. Rev. D **78**, 085003 (2008).
 - [10] D. C. Brody, Biorthogonal quantum mechanics, J. Phys. A: Math. Theor. **47**, 035305 (2014).
 - [11] F. Bagarello, R. Passante, and C. Trapani, *Non-Hermitian Hamiltonians in Quantum Physics* (Springer, New York, 2016).
 - [12] W. Chen, S. K. Özdemir, G. Zhao, J. Wiersig, and L. Yang, Exceptional points enhance sensing in an optical microcavity, Nature (London) **548**, 192 (2017).
 - [13] Z.-P. Liu, J. Zhang, S. K. Özdemir, B. Peng, H. Jing, X.-Y. Lü, C.-W. Li, L. Yang, F. Nori, and Y.-X. Liu, Metrology with \mathcal{PT} -symmetric cavities: Enhanced sensitivity near the \mathcal{PT} -phase transition, Phys. Rev. Lett. **117**, 110802 (2016).
 - [14] L. Feng, R. El-Ganainy, and L. Ge, Non-Hermitian physics and \mathcal{PT} symmetry, Nat. Photon. **11**, 752 (2017).
 - [15] R. El-Ganainy, M. Khajavikhan, S. Rotter, D. N. Christodoulides, and S. K. Özdemir, Non-Hermitian physics and \mathcal{PT} symmetry, Commun. Phys. **2**, 1 (2019).
 - [16] M. Parto, Y. G. N. Liu, B. Bahari, M. Khajavikhan, and D. N. Christodoulides, Non-Hermitian and topological photonics: Optics at an exceptional point, Nanophotonics **10**, 403 (2021).
 - [17] J. Peřina Jr. and A. Lukš, Quantum behavior of a \mathcal{PT} -symmetric two-mode system with cross-Kerr nonlinearity, Symmetry **11**, 1020 (2019).
 - [18] J. Peřina Jr., A. Lukš, J. K. Kalaga, W. Leoński, and A. Miranowicz, Nonclassical light at exceptional points of a quantum \mathcal{PT} -symmetric two-mode system, Phys. Rev. A **100**, 053820 (2019).
 - [19] E. G. Turitsyna, I. V. Shadrivov, and Y. S. Kivshar, Guided modes in non-Hermitian optical waveguides, Phys. Rev. A **96**, 033824 (2017).
 - [20] X. Xu, L. Shi, L. Ren, and X. Zhang, Optical gradient forces in \mathcal{PT} -symmetric coupled-waveguide structures, Opt. Express **26**, 10220 (2018).
 - [21] E.-M. Graefe and H. F. Jones, \mathcal{PT} -symmetric sinusoidal optical lattices at the symmetry-breaking threshold, Phys. Rev. A **84**, 013818 (2011).
 - [22] M.-A. Miri, A. Regensburger, U. Peschel, and D. N. Christodoulides, Optical mesh lattices with \mathcal{PT} symmetry, Phys. Rev. A **86**, 023807 (2012).
 - [23] M. Ornigotti and A. Szameit, Quasi \mathcal{PT} -symmetry in passive photonic lattices, J. Opt. **16**, 065501 (2014).
 - [24] T. Shui, W.-X. Yang, L. Li, and X. Wang, Lop-sided Raman-Nath diffraction in \mathcal{PT} -antisymmetric atomic lattices, Opt. Lett. **44**, 2089 (2019).
 - [25] M. Drong, M. Dems, J. Peřina Jr., T. Fordos, H. Y. Jaffres, K. Postava, and H. J. Drouhin, Time-dependent laser cavity perturbation theory: Exploring future nano-

- structured photonic devices in semi-analytic way, *J. Lightwave Technol.* **40**, 4735 (2022).
- [26] R. El-Ganainy, K. G. Makris, D. N. Christodoulides, and Z. H. Musslimani, Theory of coupled optical \mathcal{PT} -symmetric structures, *Opt. Lett.* **32**, 2632 (2007).
- [27] H. Ramezani, T. Kottos, R. El-Ganainy, and D. N. Christodoulides, Unidirectional nonlinear \mathcal{PT} -symmetric optical structures, *Phys. Rev. A* **82**, 043803 (2010).
- [28] A. A. Zyblovsky, A. P. Vinogradov, A. A. Pukhov, A. V. Dorofeenko, and A. A. Lisyansky, \mathcal{PT} -symmetry in optics, *Physics-Uspekhi* **57**, 1063 (2014).
- [29] M. Ögren, F. K. Abdullaev, and V. V. Konotop, Solitons in a \mathcal{PT} -symmetric $\chi^{(2)}$ coupler, *Opt. Lett.* **42**, 4079 (2017).
- [30] J. Naikoo, K. Thapliyal, S. Banerjee, and A. Pathak, Quantum Zeno effect and nonclassicality in a \mathcal{PT} -symmetric system of coupled cavities, *Phys. Rev. A* **99**, 023820 (2019).
- [31] B. Peng, Ş. K. Özdemir, F. Lei, F. Monifi, M. Gianfreda, G. L. Long, S. Fan, F. Nori, C. Bender, and L. Yang, Parity-time-symmetric whispering-gallery microcavities, *Nat. Phys.* **10**, 394 (2014).
- [32] B. Peng, Ş. K. Özdemir, S. Rotter, H. Yilmaz, M. Liertzer, F. Monifi, C. M. Bender, F. Nori, and L. Yang, Loss-induced suppression and revival of lasing, *Science* **346**, 328 (2014).
- [33] X. Zhou and Y. D. Chong, \mathcal{PT} symmetry breaking and nonlinear optical isolation in coupled microcavities, *Opt. Express* **24**, 6916 (2016).
- [34] I. I. Arkhipov, A. Miranowicz, O. Di Stefano, R. Stassi, S. Savasta, F. Nori, and S. K. Özdemir, Scully-Lamb quantum laser model for parity-time-symmetric whispering-gallery microcavities: Gain saturation effects and nonreciprocity, *Phys. Rev. A* **99**, 053806 (2019).
- [35] I. I. Arkhipov, A. Miranowicz, F. Minganti, and F. Nori, Quantum and semiclassical exceptional points of a linear system of coupled cavities with losses and gain within the Scully-Lamb laser theory, *Phys. Rev. A* **101**, 013812 (2020).
- [36] F. Quijandría, U. Naether, S. K. Özdemir, F. Nori, and D. Zueco, \mathcal{PT} -symmetric circuit QED, *Phys. Rev. A* **97**, 053846 (2018).
- [37] A. Guo, G. J. Salamo, D. Duchesne, R. Morandotti, M. Volatier-Ravat, V. Aimez, G. A. Siviloglou, and D. N. Christodoulides, Observation of \mathcal{PT} -symmetry breaking in complex optical potentials, *Phys. Rev. Lett.* **103**, 093902 (2009).
- [38] C. Tchodimou, P. Djorwe, and S. G. Nana Engo, Distant entanglement enhanced in \mathcal{PT} -symmetric optomechanics, *Phys. Rev. A* **96**, 033856 (2017).
- [39] D.-Y. Wang, C.-H. Bai, S. Liu, S. Zhang, and H.-F. Wang, Distinguishing photon blockade in a \mathcal{PT} -symmetric optomechanical system, *Phys. Rev. A* **99**, 043818 (2019).
- [40] R. El-Ganainy, M. Khajavikhan, and L. Ge, Exceptional points and lasing self-termination in photonic molecules, *Phys. Rev. A* **90**, 013802 (2014).
- [41] F. Minganti, D. Huybrechts, C. Elouard, F. Nori, and I. I. Arkhipov, Creating and controlling exceptional points of non-Hermitian Hamiltonians via homodyne Lindbladian invariance, *Phys. Rev. A* **106**, 042210 (2022).
- [42] M. V. Berry and M. Wilkinson, Diabolical points in the spectra of triangles, *Proc. R. Soc. London A* **392**, 15 (1984).
- [43] J. Peřina Jr., A. Miranowicz, G. Chimczak, and A. Kowalewska-Kudłasyk, Quantum Liouvillian exceptional and diabolical points for bosonic fields with quadratic Hamiltonians: The Heisenberg-Langevin equation approach, *Quantum* **6**, 883 (2022).
- [44] I. I. Arkhipov, A. Miranowicz, F. Minganti, S. K. Özdemir, and F. Nori, Dynamically crossing diabolic points while encircling exceptional curves: A programmable symmetric-asymmetric multimode switch, *Nature Commun.* **14**, 2076 (2023).
- [45] F. Minganti, A. Miranowicz, R. Chhajlany, and F. Nori, Quantum exceptional points of non-Hermitian Hamiltonians and Liouvillians: The effects of quantum jumps, *Phys. Rev. A* **100**, 062131 (2019).
- [46] F. Minganti, A. Miranowicz, R. W. Chhajlany, I. I. Arkhipov, and F. Nori, Hybrid-Liouvillian formalism connecting exceptional points of non-Hermitian Hamiltonians and Liouvillians via postselection of quantum trajectories, *Phys. Rev. A* **101**, 062112 (2020).
- [47] J. Peřina, *Quantum Statistics of Linear and Nonlinear Optical Phenomena* (Kluwer, Dordrecht, 1991).
- [48] J. Peřina Jr., On the equivalence of some projection operator techniques, *Physica A* **214**, 309 (1995).
- [49] I. I. Arkhipov, F. Minganti, A. Miranowicz, and F. Nori, Generating high-order quantum exceptional points in synthetic dimensions, *Phys. Rev. A* **101**, 012205 (2021).
- [50] J. Peřina Jr., K. Thapliyal, G. Chimczak, A. Kowalewska-Kudłasyk, and A. Miranowicz, Multiple quantum exceptional, diabolical, and hybrid points in multimode bosonic systems: II. nonconventional \mathcal{PT} -symmetric dynamics, unidirectional coupling and general genuine points, arxiv (2024).
- [51] I. I. Arkhipov, A. Miranowicz, F. Nori, S. K. Özdemir, and F. Minganti, Fully solvable finite simplex lattices with open boundaries in arbitrary dimensions, *Phys. Rev. Res.* **5**, 043092 (2023).
- [52] L. Mandel and E. Wolf, *Optical Coherence and Quantum Optics* (Cambridge Univ. Press, Cambridge, 1995).
- [53] A. Lukš, V. Peřinová, and J. Peřina, Principal squeezing of vacuum fluctuations, *Opt. Commun.* **67**, 149 (1988).
- [54] V. V. Dodonov, Nonclassical states in quantum optics: A squeezed review of the first 75 years, *J. Opt. B: Quantum Semiclass. Opt.* **4**, R1 (2002).
- [55] G. Chimczak, A. Kowalewska-Kudłasyk, E. Lange, K. Bartkiewicz, and J. Peřina Jr., The effect of thermal photons on exceptional points in coupled resonators, *Sci. Rep.* **13**, 5859 (2023).
- [56] R. W. Boyd, *Nonlinear Optics, 2nd edition* (Academic Press, New York, 2003).
- [57] W. Vogel and D. G. Welsch, *Quantum Optics, 3rd ed.* (Wiley-VCH, Weinheim, 2006).
- [58] J. Peřina Jr. and J. Peřina, Quantum statistics of nonlinear optical couplers, in *Progress in Optics, Vol. 41*, edited by E. Wolf (Elsevier, Amsterdam, 2000) pp. 361–419.
- [59] H. Hodaei, A. U. Hassan, S. Wittek, H. Garcia-Gracia, R. El-Ganainy, D. N. Christodoulides, and M. Khajavikhan, Enhanced sensitivity at higher-order exceptional points, *Nature (London)* **548**, 187 (2017).
- [60] H. Jing, S. K. Özdemir, H. Lu, and F. Nori, High-order exceptional points in optomechanics, *Sci. Rep.* **7**, 3386 (2017).